GROWTH OF UNIFORM LAYERS OF NANOSIZED ZEOLITES ON 3D ORDERED MACROPOROUS CARBON:

SYNTHESIS, CHARACTERIZATION, AND CATALYTIC EVALUATION

BY

Toufic Nabil Aridi

A Thesis Presented to the

DEANSHIP OF GRADUATE STUDIES

KING FAHD UNIVERSITY OF PETROLEUM & MINERALS

DHAHRAN, SAUDI ARABIA

In Partial Fulfillment of the
Requirements for the Degree of

MASTER OF SCIENCE

In

CHEMISTRY

MAY, 2006

KING FAHD UNIVERSITY OF PETROLEUM & MINERALS
DHAHRAN, SAUDI ARABIA

DEANSHIP OF GRADUATE STUDIES

This thesis, written by **Toufic Nabil Aridi** under the direction of his thesis advisor and approved by his thesis committee, has been presented to and accepted by Dean of Graduate Studies, in partial fulfillment of the requirements for the degree of **MASTER OF SCIENCE IN CHEMISTRY**.

Thesis Committee

Dr.Mohammed Al–Daous
Thesis Advisor

Sk. Asrof Ali
Dr. Shaikh Asrof Ali
Member

Dr. Sulaiman S.Al Khattaf
Member

Dr. Zaki Shaker Seddigi 21/5/06
Department Chairman

Dr.Mohammed Abdulaziz Al-Ohali
Dean of Graduate Studies

[Date] 28-5-2006

Dedicated to
my Mother, Father
and Brothers

ACKNOWLEDGMENT

Gratitude and praise be to Almighty Allah for making it possible for me to accomplish this work successfully.

I wish to register my gratitude and unreserved appreciation to Dr. Mohammed A.Al-Daous who served as my thesis advisor. The success of this work is credited to his endless support and priceless idea. I wish to thank the other members of my thesis committee, Prof. Shaikh Asrof Ali and Dr Sulaiman Khattaf for their constructive suggestions .

I wish to express my thanks to all faculty members and staff of chemistry department for their support.

My sincere appreciation to all of my friends at KFUPM not only for the moral support but also for their concern and encouragement in the course of my studies.

My profound gratitude and appreciation to my mother, father, brothers, relatives, and friends in Lebanon for their affection and concern.

Finally, I wish to thank King Fahd University of Petroleum and Minerals for the assistantship and support of this research.

TABLE OF CONTENTS

Page

CH 3. RESULTS AND DISCUSSION

LIST OF TABLES

LIST OF FIGURES

THESIS ABSTRACT

Name: **Toufic Nabil Aridi**

Title: **Growth of Uniform Zeolitic Layers on 3 D Ordered Macroporous Carbon : Synthesis, Characterization, and Catalytic Evaluation.**

Major Field: **Chemistry**

Date of Degree: **May 2006**

In this study the synthesis of a hybrid catalyst composed of three-dimensionally ordered macroporous carbon coated with a hydrothermally grown layer of nano-crystalline zeolite particles is proposed. The successful synthesis of such a catalyst will be followed by various physicochemical methods such as scanning electron microscopy, solid-state ^{27}Al-NMR, powder X-ray diffraction, surface area measurement, and elemental analysis of the solid catalyst. The catalyst will then be subjected to test reactions involving large guest molecules, specifically the degradation reaction of high density polyethylene (HDPE). The structure of the proposed system is expected to provide greater access to the large external surface area of acidic zeolite, thereby increasing the rate of the initial and limiting step encountered in the cracking of large polymer molecules. Moreover, the large macropores are expected to lead to the reduction in the contact time between the catalyst and the organic substrate, which could probably reduce the rate of deactivation of the external surface of the catalyst by coke; the formation of which could be the result of over-cracking of the hydrocarbon reaction-intermediates on the surface of the catalyst.

MASTER OF SCIENCE DEGREE

KING FAHD UNIVERSITY OF PETROLEUM AND MINERALS

DHAHRAN SAUDIA ARABIA

ملخص الرسالة

الاســـــــــم: توفيق نبيل العريضي

عنوان الرسالة: نمو بلورات الزيولايت على سطح كربون ذات مسام على شكل منظم ثلاثي الأبعاد: إعداد، و فحص، و تقييم نشاط الحافز.

التخصـــــص: كيمياء

تاريخ التخـرج: مايو 2006

هذه الدراسة تتضمن إعداد حافز صلب مخلوط الأجناس و مبني على الشكل التالي : قاعدة ذات مسام يتجاوز قطرها 50 nm موجودة على شكل منظم ثلاثي الأبعاد و مكون من الكربون. بعد ذلك سيتم نمو بلورات الزيولايت على سطح الكربون بطريقة التبلور الحراري المائي. سوف يتم تتبع مدى نجاح تحضير هذا الحافز بأستخدام سبل فيزائيه كيميائيه عديده مثل المجهر الإلكتروني الماسح, الرنين المغناطيسي النووي, حيود الأشعه السينيه, قياس المساحه السطحيه, وتقدير نسبة الحجم الصلب للمواد المكونه للحافز. بعد ذلك سوف يتم تقييم نشاط الحافز في تفاعلات يُستخدم فيها جزيئات ذات حجم كبير مثل البولي إثيلين ذو الكثافة العاليه. من المتوقع ان الشكل التركيبي للحافز قد يساعد على الأستفادة إلى حد أكبر من مساحة السطح الخارجي للزيولايت الحامضه, مما قد يؤدي إلى زيادة معدل التفاعل الأولي في سلسة التكسير الحفزي للبلاستيك , ومن المتوقع أن وجود المسام ذات الأقطار الكبيره قد يؤدي إلى إنخفاض زمن التلامس بين المادة العضوية و سطح الحافز, مما قد ينتج عنه تقلص في معدل خمول الحافز بسبب تكوين الفحم (الكوك) على السطح الخارجي للحافز و الذي يتكون نتيجة التكسر المتزايد للمواد الهيدروكربونيه الثنائيه على سطح الحافز.

درجة الماجستير في العلوم

جامعة الملك فهد للبترول و المعادن

الظهران- المملكة العربية السعودية

CH : 1

Introduction, Literature Review &

Objectives

1.1 - Introduction

The chemical industry today stands at a crossroad since its traditional source of hydrocarbons and petroleum has a doubtful future for a reason that the necessity of "old "petrochemical producers to remain competitive has never been as strong. To stay competitive, they have revamped plant to make it more energy and feed stock efficient, and this process will continue. However, sooner or later ,new feed stocks will have to be sought for processing to produce chemicals. This trend has already started, in the united states coal is being converted into methanol, acetic acid, and acetic anhydride by synthesis gas . In all likelihood the remainder of this century will see a growth in this process requiring new catalysts and supports. Coal for instance is a giant aromatic molecule , what could be more logical than to convert it directly into benzene, toluene, and xylene rather than indirectly into synthesis gas , methanol , and so forth [1].

To process the new macromolecules will require supports with much larger, less tortuous pores than present supports. In the area of carbon supports many attempts have been made seeking the production of mesoporous (pore diameter $2 \leq X \leq 50$nm) materials on top of which nano sized zeolites or metals are dispersed [2-6] .

In our case we propose to push it even further to higher limits and process porous supports in the macro pore size range , that permits penetration of larger guest molecules into the porous host structures , thus overcoming pore size limitations that are present in the micro and mesopore ranges .

Attempts of growing zeolites on porous supports have been widely investigated in order to prepare mesoporous zeolites [2, 4, 6] and in most of them the zeolite growth was and still not very much clarified in almost all of these attempts .In this study a uniform layer of zeolites will be grown hydrothermally on a three dimensionally ordered macroporous (3DOM) carbon assisted by a polyelectrolyte layer to overcome or break the barrier between the hydrophobic nature of the carbon and the hydrophilic nature of the zeolite chemistry .

Most research in the process of plastic degradation of plastics to fuels and valuable products, has focused on catalytic degradation. Sakata et al studied the catalytic degradation of polypropylene (PP) and polyethylene (PE) by an acidic silica-alumina catalyst in a semi-batch reactor[7]. It was found that silica-alumina was effective in increasing the degradation rate and yield of oil products in comparison to the pyrolysis of the polymer. However, such a system exhibited poor conversion caused by rapid

deactivation by carbon deposition [8] . In order to overcome such problems in catalytic polymer degradation, zeolites were proposed as a solution because of their micropores (pore diameter $\leq$ 2 nm) with specific shapes that suppress the formation of large molecules, that may act as precursors for carbon deposits[9, 10]. For example, the bent pores found in BEA and MFI zeolites are effective in preventing the formation of large hydrocarbons, extending catalyst lives and achieving high conversion [11]. Moreover Dwyer et al have identified the limiting step in polymer degradation reaction to be the initial cracking reaction of the polyolefin chains on the external surface of the zeolite crystals. Therefore there is a potential advantage in synthesizing a zeolitic structure which would provide a greater access to the zeolite particle's large external surface area to the rather bulky polymer chains.

Zeolites are microporous crystalline solids with well - defined structures. Generally they contain silicon, aluminum and oxygen in their framework and cations, water and/or other molecules within their pores .

Zeolite molecular sieves are widely used in many chemical and physical processes such as heterogeneous catalytic reactions and gas separations [12]. Synthetic zeolites have been used either separately in bulk pellets and blocks or embedded in matrices as a part of composite materials [13, 14]. Both of these forms have some drawbacks. When zeolites are used in bulk form, a large part of the zeolite is in the interior and may not be readily accessible for reactions; while in the composite form, with the zeolite encapsulated in a matrix, the effective reaction surface is reduced substantially. Greater utilization of the

zeolite surface may be achieved by depositing the zeolite on an appropriate substrate. Zeolite deposition can be accomplished either by using an adhesive substance where pre-made zeolite crystals are attached to the substrate by a coating process [15, 16], or hydrothermally growing a uniform layer of zeolites on the substrate. However because of their interpenetrating pore channels in the molecular size range of 0.3 – 1.5 nm, these materials are subject to diffusion limitations that restrict substrate accessibility to active sites on the interior surface as well as a high back – pressure on flow systems.

In order to satisfy the need for new supports with much larger and less tortuous supports, two approaches have been investigated in an effort to improve accessibility in zeolites; one is by decreasing the zeolite crystal size from the conventional micrometer to the nanoparticle size so as to increase the external surface area and reduce the diffusion path length [17-20], and the other goal involves structural control in order to increase the size of pores to permit penetration of larger guest molecules into the porous host structures.

At present several new techniques are being developed to achieve mesoporous (diameters up to 50 nm) and macroporous (diameters > 50 nm) solids with relatively narrow pore size distributions.

Recent synthesis of colloidal crystal templated 3DOM materials [15, 16] offers a potentially new catalytic supports that could be effective in processing large guest molecules, such as those found in the heavy petroleum fraction or polymers. 3DOM materials form a class of porous solids composed of several layers of close-packed air voids typically exceeding 100 nm in diameter surrounded by smooth, spherical walls and

interconnected through windows to form the 3DOM structure as shown in figure 1.1. These 3DOM materials offer additional advantage where zeolite coatings would produce composite/hybrid catalysts with large interconnected pores and large accessible surface area. These characteristics can be used to ensure good mixing of reactants in some important catalytic applications such as the degradation of the main components of polymer waste polyethylene (PE) and polypropylene (PP).

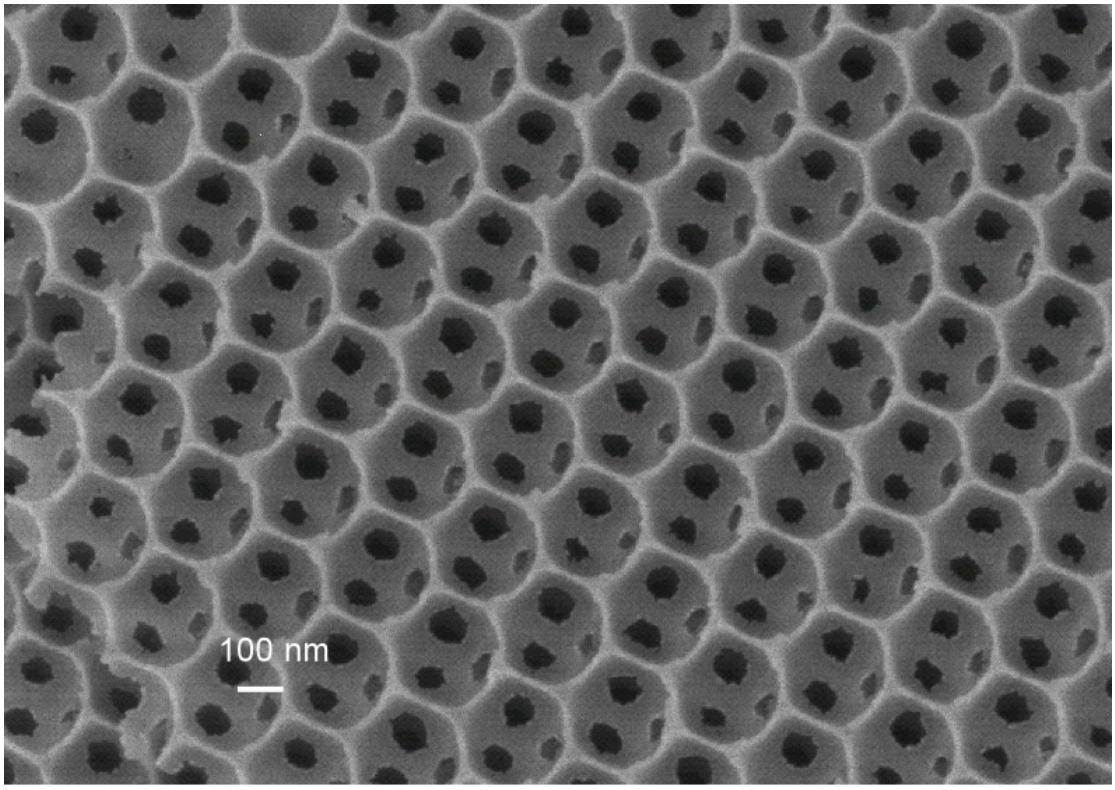

Figure 1.1 : SEM image of a 3 DOM carbon structure .

1.2 - Background & Literature Review :

1.2.1 - Zeolites :

Zeolites are microporous (pore diameter ≤ 2nm) crystalline solids with well- defined structures. Many occur naturally as minerals, and are extensively mined in many parts of the world. Others are synthetic, and are made commercially for specific uses, or produced by research scientists trying to understand more about their chemistry [21]. Because of their unique porous properties, zeolites are used in a variety of applications with a global market of several million tones per annum. They are often also referred to as *molecular sieves*. Zeolite molecular sieves are widely used in many chemical and physical processes such as heterogeneous catalytic reactions and gas separations [12]. Zeolites represent a continuously growing family of natural and synthetic microporous crystalline oxide materials with different framework structures, chemical compositions, crystal sizes, and morphologies [22].

Such microporous materials admit molecules below a certain size into their extensive internal space, which makes them widely used in purification & separation where the shape-selective properties of zeolites are also the basis for their use in molecular adsorption. The ability to preferentially adsorb certain molecules, while excluding others, has opened up a wide range of molecular sieving applications. Sometimes it is simply a matter of the size and shape of pores controlling access into the zeolite. In other cases different types of molecules enter the zeolite, but some diffuse through the channels more

quickly, leaving others stuck behind, as in the purification of *para*-xylene by silicalite [23-25].

Cation-containing zeolites are extensively used as desiccants due to their high affinity for water, and also find application in gas separation, where molecules are differentiated on the basis of their electrostatic interactions with the metal ions. Conversely, hydrophobic silica zeolites preferentially absorb organic solvents.

Zeolites can thus separate molecules based on differences of size, shape and polarity. Zeolites have the ability to act as catalysts for chemical reactions which take place within the internal cavities. An important class of reactions is that catalyzed by hydrogen-exchanged zeolites, whose framework-bound protons give rise to very high acidity. This is exploited in many organic reactions, including crude oil cracking, isomerisation and fuel synthesis. Zeolites can also serve as oxidation or reduction catalysts, often after metals have been introduced into the framework. Examples are the use of titanium ZSM-5 in the production of caprolactam, and copper zeolites in NOx decomposition [21] .

Zeolites also have the ability to act as ion-exchangers where the loosely-bound nature of extra-framework metal ions (such as in zeolite NaA) means that they are often readily exchanged for other types of metal when in aqueous solution. This is exploited mainly in water softening processes, where alkali metals such as sodium or potassium prefer to exchange out of the zeolite, being replaced by the "hard" calcium and magnesium ions from the water. Many commercial washing powders "detergents" thus contain substantial amounts of zeolite. Commercial waste water containing heavy metals, and nuclear

effluents containing radioactive isotopes can also be cleaned up using such zeolites[21, 23-26] .

Underpinning all these types of reaction is the unique microporous nature of zeolites, where the shape and size of a particular pore system exerts a steric influence on the reaction, controlling the access of reactants and products. Thus zeolites are often said to act as *shape-selective catalysts*. Increasingly, attention has focused on fine-tuning the properties of zeolite catalysts in order to carry out very specific syntheses of high-value chemicals e.g. pharmaceuticals and cosmetics .

The framework of zeolites is an extensive three dimensional network composed of silica, alumina , and oxygen in a tetrahedral fashion such that the oxygen at each tetrahedral corner is shared with that of identical tetrahedral containing either silica or alumina in its center as shown below in Figure 1.2.

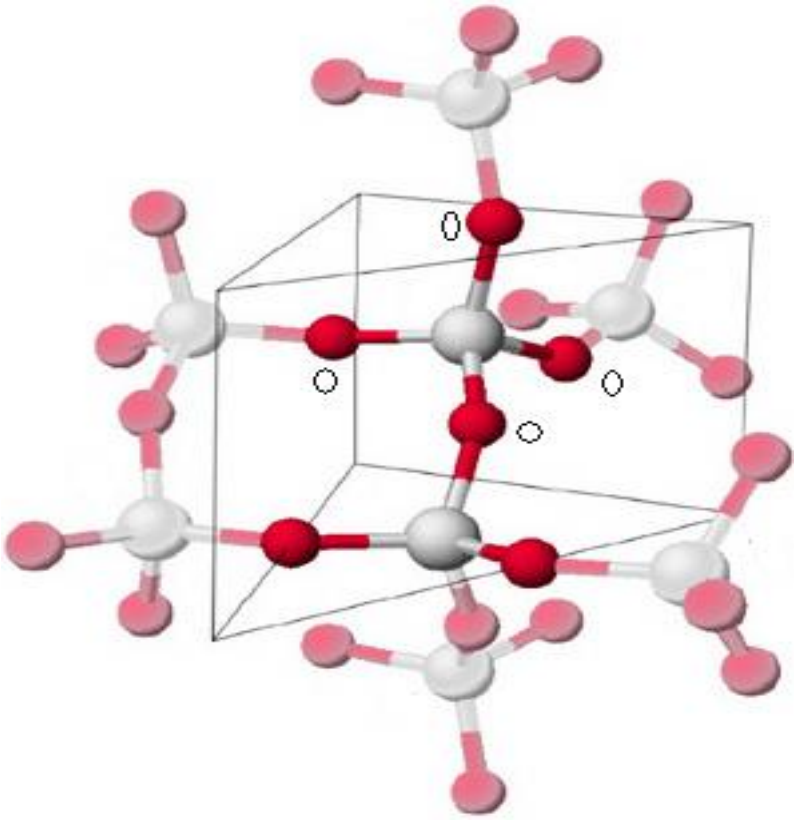

Figure 1.2 : Tetrahedral unit of silica surrounded by four oxygen atoms

The tetrahedral units form cages and channels of molecular dimensions Figure (1.3), and the (-2) oxidation state of each oxygen is accounted for as follows: each silicon ion has its (+4) charge balanced by the four tetrahedral oxygens and the silica tetrahedral are therefore electrically neutral while each alumina tetrahedral has a residual charge of (-1) since the trivalent aluminum is bonded to four oxygen anions. To maintain electrical neutrality, this negative charge on aluminum tetrahedral has to be compensated by the presence of an added positive charge. When this positive charge is H+, gives rise to the acidic character of zeolites.

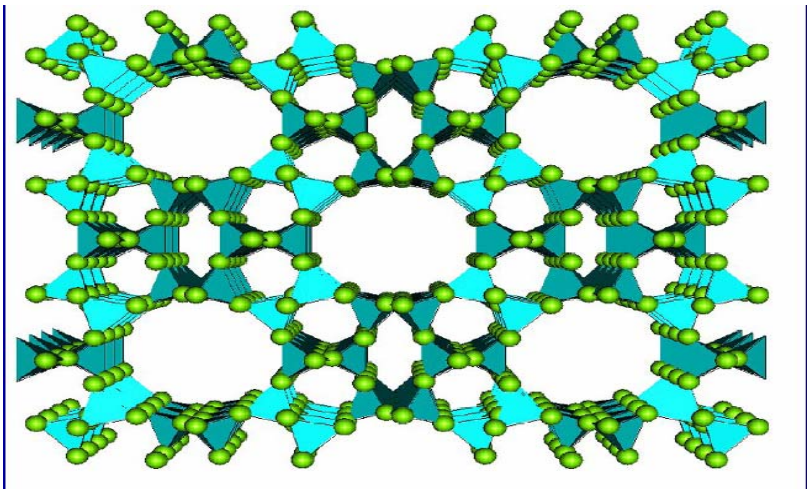

Figure 1.3 : Tetrahedral Units silica alumina and oxygen forming cages .

Zeolite synthesis :

The reduced size and dimensions in nanophase materials is at the basis of unique applications in microelectronics, nanocomposites, ultrathin oxide films, and so forth [27]. In the field of synthetic zeolites, there is also a considerable interest in decreasing the particle size from micrometer to the nanometer scale in order to decrease, for instance, mass and heat transfer resistances in catalytic and sorptive processes. The conventional hydrothermal gel method of zeolite synthesis, introduced by Barrer [28], yields typically micrometer-sized crystals.

The synthesis of zeolites was also achieved by using clear solutions instead of gels [29-31]. From clear solutions, nanocrystals of a variety of zeolite materials including silicalite-1 [32-34], Na –ZSM -5 [35], and many others have been synthesized. The

nanosized and microsized materials have many common properties including the refined structure and the nature and concentrations of structure directing agents such as tetrapropylammonium species incorporated during the synthesis of MFI morphology. Unique properties of the nanophase silicalite include the splitting of the characteristic framework vibration at 550 cm^{-1} into a doublet at 555 cm^{-1} and 570 cm^{-1}, a high concentration of defect sites, and a strain in the crystallites along the "a" crystallographic direction. Jacobs et al [36] Synthesized a silicalite-1 nanophase material with an elementary particle size of 18-100 nm from clear solution and isolated and purified using centrifugation. The synthesized form of the sample contained TPAOH on its external surfaces and TPA occluded in the micropore system. In addition to that XRD, SEM, HRTEM, and AFM showed that several properties are not different from larger crystals.

A crucial aspect of zeolites syntheis is its nucleation stage. It is also a poorly understood phenomenon, where several recent reports dealing with this area of zeolite synthesis have shown that very small colloidal particles, < 10 nm , are present in precursor solutions both prior to and throughout the course of crystallization [34, 37-39]. Since it has been estimated that the size of the critical nucleus is of the order of several unit cells [40, 41], the question as to the role of the sub–colloidal particles in the nucleation process arises . Numerous silica sources may be employed to make up a TPA- Silicalite-1 precursor solution such as Aerosil, Fumed silica, Silicic aid, and TEOS. The addition of these silica sources to a TPAOH solution, yields precursor solutions in which preformed solid amorphous silica particles exist in suspension. The role of colloidal silica particles formed in situ is believed to be more than simply supplying the growing silicalite-1 crystals with

nutrients [42]. Schoeman et al [43] studied the characterization of these particles using a modified method in which the reaction rate of monomeric silica with molybdic acid was recorded, along with light scattering studies, and cryo-TEM analysis .It was shown that sub-colloidal particles with an average size of 3 nm formed by the hydrolysis of TEOS in the presence of the structure directing agent, TPAOH, existed in silicalite-1 precursor suspensions both prior to hydrothermal treatment and during the course of crystallization. An in situ laser light scattering of TPA - Silicalite-1 yielded results indicating that the role of the sub colloidal particles may be as growth centers : either the sub colloidal particles grow to larger sizes or certain fragments of their surface may act as a " nuclei " .

Martens et al [44] studied the mechanism of transformation of precursors into nanoslabs in the early stages of MFI and MFL zeolites formation from TPAOH –TEOS-H_2O and TBAOH-TEOS- H_2O mixtures. Silicalite particles were formed upon gradual addition of TEOS to concentrated TPAOH and TBAOH solutions, and then dilution of the concentrated solution with water .The formed sub colloidal particles are called nanoslabs with very specific dimensions and with the MFI framework connectivity [45]. In the TBAOH system almost 90% of the nanoslabs are converted into intermediates composed of two nanoslabs, since only one step is necessary to reach the product, the reaction is found to be faster than with TPAOH where in the TPAOH system and after addition of water the volume of nanoslabs and smaller particles decreases in favor of intermediates until 30% of the nanoslabs are converted into intermediates for which the final intermediate is the product of multiple aggregations involving also difficult linkages along the large faces of the slabs. The silicate particles were studied in situ X-ray scattering

(XRS) and gel permeation chromatography (GPC). Heating of the clear solution shifts the equilibria of nanoblocks and intermediates toward the aggregates which then form the final product of the solution synthesis .

Although zeolites are widely use as catalysts and adsorbents little is known about the crystallization mechanisms of these microporous solids. The zeolite silicalite-1 with MFI topology first reported by Flanigen et al [46] in the early 70s can be synthesized either by the traditional hydrothermal gel method or from a so- called "clear solution " [35, 47, 48].Many studies on the gel and clear solution processes were undertaken to elucidate the mechanism of MFI synthesis .By now a step wise mechanism seems to be emerging from these efforts : the initial formation of a precursor leads to the formation of a nanoscopic species with well defined size. These entities already are observed before heating the reaction mixtures and are present during the formation of a growing fraction of final crystals at elevated temperatures. Martens et al [49]studied the silica species contained in an aged clear suspension, which upon heating gives rise to the crystallization of slicalite-1. These species were extracted with 80 % efficiency using a sequence of acidification, salting out, phase transfer into organic solvent, and freeze drying methods. The extracted solid can easily be redispersed in water to give a clear liquid, containing nanoblocks of the same size as before . Martens et al [49]studied the characterization of this silica powder by X-ray scattering, transmission electron microscopy, atomic force microscopy, and ^{29}Si image angle spinning nuclear magnetic resonance .

The detailed molecular mechanisms of nucleation and growth of zeolite crystals and the effect of templates on these processes remain unclear .Recent ^{29}Si NMR studies on tetraalkylammonium silicate solutions [50] demonstrated the tremendous influence of these templates on the formation of polysilicate anions. The smaller alkyl groups, as in tetramethyl ammonium, direct the system toward small, closed, cage like structures, whereas the larger alkyl chains favor the formation of more open structures. The key for understanding the successive steps is the hydrophobic surface of the propyl chains of the TPA, which tend to sheath in siliceous gloves [50-52] while the TPA cation as a whole strains for the charge compensation. The bicyclic pentamer , the pentacyclic octamer , and the tetracyclic undecamer represent a growing curved hydrophobic SiO_2 surface with all hydroxyl groups pointing outward .Thus a bifunctional interface with an outer hydrophilic and an inner hydrophobic surface is created. Zeolites with the MFI framework topology are members of the pentasil family which have in common that their framework structures are built from five-membered rings [53] .

Novel Zeolite synthesis processes are normally optimized to obtain a product of specific properties and/or to identify optimum commercial conditions for the production of zeolite. In his case when the zeolite catalytic activity or the sorption characteristic are sensitive to the method of synthesis, these normally take priority, and the synthesis method is optimized accordingly. On the other hand, when the zeolite properties are not sensitive to the method of the synthesis, both the manufacturer and the end user have interest in optimizing the manufacturing procedure to reduce the production cost .Such optimization often involves the study of many variables including the composition of the hydrogel, the

method of its preparation , and the conditions of zeolite crystallization .In this direction of MFI-type, zeolites were synthesized by Inui [54] using the rapid crystallization method in two hours. Investigation of the rapid crystallization method for synthesis of MFI-type zeolites and study of the physiochemical properties of the products was investigated by Ahmed et al [55] where ZSM-5 zeolites were synthesized and the thermal stability was found to decrease with increasing Si/Al ratio contrary to what was widely accepted. It was speculated that high concentrations of defect sites exaggerated by the rapid crystallization time may be responsible for the trend of thermal stability.

1.2.2 - Mesoporous materials

Zeolites and zeo-type phases are used extensively to catalyze a number of chemical reactions in refinery and petrochemical processing [56].Owing to their microporous channel structures (pore sizes < 2nm) and monolithic particle morphology, these materials are subject to diffusional limitations that restrict substrate accessibility to active sites on the interior surfaces. Several approaches are currently being investigated as possible solutions to this limitation. For instance, new generations of mesostructured aluminosilicates, such as those represented by the M-41 S family of materials [57], are being developed with pore sizes > 2 nm .Also the diffusion length into the framework structure of conventional zeolite crystals is being reduced through the introduction of extra framework mesoporosity using various postsynthesis treatment methods [58, 59]. In addition, mesopores have been introduced in zeolite crystals by occluding small (12 or 18

nm) nanosized carbon particles or macromolecules into crystals during synthesis and subsequently removing through oxidation [60-62].

As an alternative to forming new mesostructures or to creating mesoporosity in zeolitic crystals, another possibility is to decrease the crystal size of a zeolite thereby increasing the external surface area and reducing the diffusion path length. Nanosized zeolites have received much attention in catalytic applications including Fluid Catalytic Cracking (FCC), hydrocracking of gas oil, hydroxylation of phenol, and the hydration of cyclohexene to cyclo hexanol [63-66]. ZSM-5 with an average particle size of 30 nm exhibited reduced deactivation through coke formation in the catalytic aromatization of ethylene [67]. Efforts to prepare ZSM-5 particles with an average size smaller than 8 nm have resulted in the formation of X-ray amorphous products [68].

Recently nanosized ZSM-5 crystals have been prepared by crystallizing the zeolite in the void spaces of a carbon black and then removing the carbon by combustion in air [69]. Mesoporous carbons with much more uniform pore size distributions can be formed through the carbon replication of mesostructured silicas [70] and through the colloid imprinting of pitch [71].In comparison to carbon blacks , other forms of carbon with more uniform pore sizes are considered to be more suitable templating media for the "nanocasting" [72] of zeolite phases. In that regard Pinnavaia et al [73] used colloid-imprinted carbons (CIC) with average pore size in the range of 12, 22, 45, and 85 nm as templates for the nanocasting of ZSM-5 zeolite with spherical domain sizes comparable to the pore sizes of the CIC template. The size and shape fidelity of the CIC nanocasted

zeolite allows one to control both the external surface area and the interparticle mesopore volume through a rational choice of the template pore size. This felxibilty in tailoring the particle textural properties makes it possible to optimize the catalytic processes of the zeolite for the conversion of molecules that are too large to penetrate the framework micropores and constrained to reacting only at active sites on the external particle surfaces. Conversely, for small molecule conversions within the framework micropores, the nanocasting method allows uniform tailoring of the diffusion path length to optimize reactivity or selectivity.

Mokaya et al [74] synthesized ZSM-5 zeolites with unique supermicropores using mesoporous carbon as a template, the preparation of these zeolites was obtained by synthesizing the zeolite using well-ordered mesoporous carbon (CMK-3) as the solid template which in turn is prepared by calcinations of mesoporous SBA-15 silicas.The porosity of the resulting mesoporous ZSM-5 materials can be tailored so as to include micropores , supermicropores /small mesopores, and large mesopores by simply changing the nature of the mesoporous carbon template.

Kaneko et al [75] prepared Zeolites of tunable mesoporosities by using Resorcinol-Formaldehyde aerogels and carbon areogels of different mesoporsities as templates, which in turn were synthesized from a sol-gel polymerization process of resorcinol and formaldehyde. The formation of the highly crystalline zeolitic forms of mesoporous zeolites is supported by XRD and FT-IR spectra, and the invariant basic cell structure is

indicated by ^{29}Si MAS NMR .Their mesoporosities are evidenced by adsorption analysis as well as FE- SEM observation.

Boisen et al [76] synthesized mesoporous zeolite single crystals with an MFI morphology by carbon nanotube templating and later characterized these mesoporous zeolite single crystals with intracrystalline mesopores and metal oxide particles located in the zeolite mesopore by TEM stereo-imaging .

In comparison to crystalline microporous zeolites , mesoporous aluminosilicates lack hydrothermal stability and strong acidity due to their non-crystalline framework walls. Significant improvements in both the hydrothermal stability and acidity of mesostructured aluminosilicates have been recently reported by pinnavaia et al [77] .The most promising strategy for improving these properties of aluminosilicate mesostructures, is based on the use of proto-zeolitic nanoclusters. These so called "zeolite seeds" can be directly assembled into hexagonal, cubic ,wormhole, and foamlike framework structures under a variety of assembly conditions.They can also be grafted into the walls of pre-assembled frameworks to form more stable acidic derivatives.The improved hydrothermal stability is achieved by thickening the walls, whereas the acidity was enhanced by introducing tetrahedral AlO_4 into the framework .

1.2.3 - Macroporous Materials

One goal in structural control has been to increase the size of pores to permit penetration of larger guest molecules into the porous host structures. Until the advent of MCM-41 and related mesoporous materials, pore sizes in ordered structures were limited, with few exceptions, to a range below 2 nm [78] .In mesoporous solids, structural order and pore size control has been achieved by employing micellar arrays of surfactant molecules as structure-directing agents in a cooperative assembly process between the organic and inorganic species used .At present several new techniques are being developed to achieve even larger mesoporous (diameter up to 50nm) and macroporous (diameter > 50nm) solids with relatively narrow pore size distributions.The condensation of a silicate network within a triblock copolymer structure and subsequent extraction of the polymer resulted in periodic mesopores with 5-30 nm diameters [79]. Macropores with diameters of a few hundred nanometers have recently been templated in inorganic solids by latex sphere dispersions in the presence of surfactants [80] and by oil/formamide emulsions [81, 82]. Although these materials can have relatively narrow pore size distributions, their structural periodicity in three dimensions have been limited. Greater order has been achieved in macroporous thin silica films that were templated by surfactant-modified latex spheres deposited on a membrane as 10 micrometer thick colloidal crystals [83]. In that regard Stein et al [84] synthesized highly ordered, three dimensional, macroporous materials in a straight forward single step reaction. Monodisperse polystyrene latex spheres were ordered into close-packed arrays by centrifugation.The interstices between the latex sphere were permeated by inorganic solution that can be made up of Si, Ti, Zr, Al, W, Fe, and Sb; that subsequently hydrolyze and condense in the void spaces. An

inorganic framework was formed upon drying. Removal of the latex spheres was accomplished by either calcination at temperatures between 450 and 1000 °C or extraction with a tetrahydrofuran/acetone mixture. The resulting products consisted of periodic, interconnected networks of monodisperse submicron pores extending over hundreds of micrometers. Depending on the technique of template removal, various phases of the inorganic oxide could be formed. The synthesis has also been expanded to other compositions including aluminophosphates and hybrid organosilicates, as well as silicates with bimodal distributions of meso- and macropores. These structures could potentially find applications as chromatographic support materials, solid catalysts, battery materials, thermal insulators, or photonic crystals.

Stein et al [85] also presented a general method to prepare three-dimensionally ordered macroporous (3DOM) metal oxides or carbonates via templating with polystyrene (PS) spheres. The method is based on templated precipitation of metal salts (acetates, oxalates, oxides) within a colloidal crystal of PS spheres and subsequent chemical conversion of the inorganic precursors. The compositional range of possible macroporous products includes oxides or carbonates of many metals in the periodic table e.g., MgO, Cr_2O_3, Mn_2O_3, Fe_2O_3, Co_3O_4, NiO, ZnO, $CaCO_3$, including compositions that are less accessible or more expensive by previous syntheses based on metal alkoxide precursors .In this process liquid metal alkoxides, either neat or in solution, were first introduced into the spaces between the templating sphere array; subsequently a solid metal oxide skeleton was constructed via in situ sol-gel transformation, which maintained its shape after the templating agents were removed. However, this method is most suitable for the

preparation of high valence metal oxides. For many low-valence transition metal oxides and alkaline earth metal oxides, the formation of an ordered 3D framework becomes more difficult, if the alkoxide precursors hydrolyze/polymerize too rapidly to fill the voids in the template, or if they have a low solubility in a solvent that is compatible with the template array. Moreover, the high cost and difficulty of obtaining certain metal alkoxide precursors commercially hinder research progress in the fabrication of these important functional materials with 3DOM structures. Regardless of the precursor, the template material, and the template packing or removal methods, the key point of the colloidal crystal templating method lies in the design of a fluid-solid transformation which takes place in the interstices of the colloid crystals.

1.2.4 – Catalytic degradation of Polymers :

The huge amounts of waste plastics give rise to serious environmental concerns. Plastic does not degrade and remains in municipal refuse tips for decades. During the past few years recycling of plastics has been recognized as a necessity. Polymer recycling methods can be grouped as follows :

a - Mechanical reprocessing of the used plastics to form new products.This method has found very limited application, as it is not generally applicable because of the low quality of new products and the need for pure waste plastic streams.

b - Incineration of the plastics to recover energy. This method produces toxic gaseous compounds and only shifts a solid waste problem to one of air pollution .

c - Thermal and/or catalytic degradation of plastic waste to gas and liquid products, which can be utilized as fuels or chemicals. These methods seem to be the most promising to be developed into a cost-effective commercial polymer recycling process to solve the acute environmental problem of plastic waste disposal.

The products of pure thermal degradation show a wide product distribution of carbon numbers requiring further processing of their quality to be upgraded [86, 87].Catalytic degradation on the other hand yields a much narrower product distribution of carbon atom number with peak at lighter hydrocarbons [11, 88-90].

Dwyer et al [91] studied the catalytic degradation of high density polyethylene over ultrastable Y zeolite in a semibatch reactor at different heating rates and reaction temperatures. The catalytic degradation of the polymer occurred at much lower temperatures than pure thermal degradation. The catalyst showed that its presence was necessary to initiate solid-state reactions that changed the polymer structure mainly by the breaking of chains of low smaller molar mass chains. These results indicated that the homogenous pure thermal degradation was a kinetically controlled reaction, albeit requiring much higher activation, while the catalytic one occurred at lower temperature, but was limited by a slow initial macromolecule breaking step. It is reasonable to assume that large macromolecules had to react on the external surface of the zeolite catalyst first which could be the limiting reaction step.

Seo et al [92] studied the liquid-phase catalytic degradation of polyethylene wax into fuel oil was studied over MFI catalysts with different particle sizes. Although structures and

acidities of these catalysts were almost the same, the degradation activity varied greatly according to their particle size. The small particle catalyst showed higher activity due to its larger external surface, and to the low restriction on the mass transfer of large polymer molecules .Since carbon deposits are severe in liquid-phase degradation, MFI zeolite is particularly suitable for investigating the contribution of the external surface to their catalytic activity. Its particular pore shape with its sinusoidal structure prevents the formation of large molecules , thus reducing carbon deposit in the pore and sustaining its catalytic activity. The product distribution was also dependent on the particle size, producing higher hydrocarbons in the liquid product on the catalyst of small particles.

1.3 - Objectives :

The objectives of this study can be divided into three main parts :

1- The synthesis of 3DOM modified carbon substrate, on top of which a uniform layer of nano-crystalline ZSM-5 or NaY zeolites will be grown hydrothermally .

2- Investigating physicochemical properties of the resulting product by conducting essential characterization techniques such as scanning electron microscopy, surface area and pore volume measurement, thermogravimetric analysis, infrared spectroscopy, ICP, powder X-ray diffraction, and ^{27}Al and ^{29}Si solid-state NMR .

3- Various catalytic reactions will also be conducted to investigate the effect of the 3DOM structure and the role of the catalytic surface on the reaction. The catalyst will then be applied in the cracking of model high density polyethylene.

CH: 2

Experimental Methods

2.1 - Synthesis

The particular structure sought is that of a 3DOM scaffold composed of modified carbon uniformly coated with nano-crystalline ZSM-5 zeolites .

Synthesis of the proposed 3DOM catalyst requires the preparation of a colloidal crystal template from a non-crosslinked poly (methyl methacrylate) monodisperse latex dispersion which is later collected and dried .The latex then is soaked with a carbon precursor solution for few minutes , followed by drying the composite and then calcining it in inert atmosphere .After the 3DOM carbon is prepared nano sized ZSM-5 zeolites are grown on the walls of the 3DOM .

2.1.1 Colloidal Crystal Template synthesis :

The first step in the synthesis of the catalyst involves the preparation of the colloidal crystal template from a non-crosslinked poly(methyl methacrylate) monodisperse latex dispersion, which can be synthesized using an emulsifier-free emulsion polymerization

technique. Into a five necked round bottom flask which is hooked to a condenser, stirrer, thermocouple ,gas flow, and heat controller, was added distilled water and methyl methacrylate monomer in a volume ratio of 2: 1 and left stirring at 65 ^{0}C for three hours in order to remove the inhibitor. After that an initiator was added and emulsion polymerization took place forming monodisperse latex spheres suspended in solution . Before use, the spheres need to be close-packed into colloidal crystals by either gravity sedimentation or centrifugation followed by drying at room temperature.

2.1.2 Synthesis of the 3 DOM carbon:

The 3DOM carbon is prepared using a clear liquid containing resorcinol as the carbon source and formaldehyde in a ratio of 1 to 9 in addition to few grams of sodium carbonate. The prepared solution is used to soak the dried latex for few minutes, followed by filtering the excess solution and drying the composite at room temperature for about 24 hours. The 3DOM is then formed as shown in Figure 2.1 by heating the latex/resorcinol composite in flowing nitrogen at 600-625 °C for 2-3 hours. The later process is called calcination and serves two purposes; one is the removal of the latex and the other is to carboryze the resorcinol.

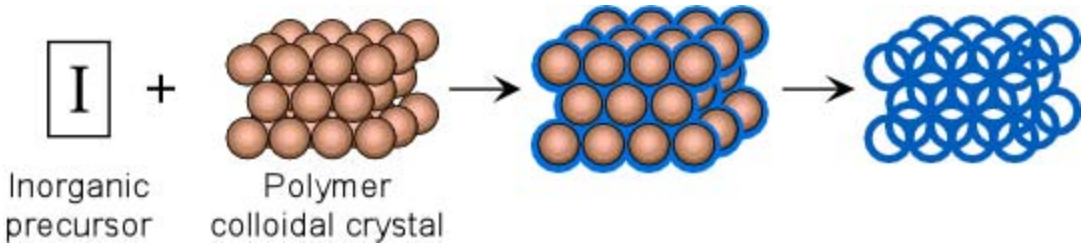

Figure 2.1 : Schematic sketch of 3 DOM preparation .

2.1.3 Titration of the 3 DOM carbon

The prepared 3DOM structure was titrated in order to determine the pH at which the surface charge of carbon is zero. The titration procedure was done by preparing three salt solutions with different ionic strengths:

- Solution (1) : 0.1 M KNO_3 solution composed of 50% water and 50% ethanol as a wetting agent for the carbon which will be later soaked in this solution .

- Solution (2) : 0.01 M KNO_3 solution composed of 50% water and 50% ethanol as a wetting agent for the carbon which will be later soaked in this solution .

- Solution (3) : 0.001 M KNO_3 solution composed of 50% water and 50% ethanol as a wetting agent for the carbon which will be later soaked in this solution .

In addition to these solutions 0.1 M solutions of KOH and HNO_3 were prepared as follows :

- 0.1 M KOH solution : 0.56 g of KOH were dissolved in 100 ml of H_2O and then the prepared solution was titrated with a potassium hydrogen phthalate (KHP) solution , 0.350 g KHP and 50ml of H_2O, in order to determine the exact concentration of the KOH solution .

- 0.1 M HNO_3 solution : 0.96 g of a 65 % HNO_3 solution were added to a 100 ml flask and filled with distilled water to the marker. The prepared solution was titrated with the previously prepared and titrated KOH solution in order to know the exact concentration of the HNO_3 solution .

After all solutions were prepared, combinations of these solutions with 0.15 g of the 3DOM carbon added to each vile were prepared.

The vials were left stirring for two days, after which the pH of the whole solution was measured and a plot of the volume of acid and base versus the pH was taken for each class of the three salt solutions. The point of intersection of all three curves is the point of zero charge which was found to be at a PH of 4. Thus in order to grow zeolites on the carbon surface an interface between the negatively charged zeolite precursor solution and the negatively charged carbon should exist for growth to take place. This is accomplished by coating the carbon surface by a polyelectrolyte layer starting with a positive layer since our carbon is negative and then followed by a negative layer and so on, this procedure was done several times with the last polyelectrolyte layer being positive is coating the carbon surface .

2.1.4 Synthesis of ZSM-5 precursor solution :

Molar composition:

2.5 Na_2O :14 TPA Br : Al_2O_3 : 30SiO_2: 400 H_2O

The zeolite precursor mixture was prepared by dissolving 1.3329 of sodium aluminate ($NaA10_2$), 0.6679 of sodium hydroxide, and 7.1023 of tetrapropyl ammonium bromide (TPABr) in 30.00g of distilled water. 30.00gram of the colloidal silica (Ludox AS-40) was added drop wise under continuous stirring. The resulted solution was stirred to homogeneity under magnetic stirring for 12 hours. Then, the homogeneous solution became ready to act as a precursor for growing the zeolites on the 3 DOM walls or to prepare powdered zeolites .

2.1.5 Synthesis of powdered ZSM- 5 zeolites

The as-synthesized precursor solution as prepared in 2.1.3 is introduced into a 40 ml autoclave and heated at 150 ^{0}C for 24 hours. The material is left to cool down, then filtered and washed with distilled water. The collected zeolite powder was left to dry in the oven at 100 ^{0}C .

2.1.6 Calcination of the powdered ZSM-5 .

The as-synthesized powdered zeolites in 2.1.4 still contains the TPABr in its pores blocking it, thus calcination of the obtained material at a rate of 1 ^{0}C/minute up to 550 ^{0}C is performed in order to get rid of the TPABr and open the pores of the zeolites .

2.1.7 Growth of a nano sized ZSM-5 layer on 3DOM carbon .

The prepared 3DOM carbon already coated with the polyelectrolyte layer was soaked in the clear zeolite precursor solution as prepared in 2.1.3 in a 40 mL autoclave at room temperature for 24 h and later followed by heating at 100 °C for 48 h in an autoclave oven. Then the sample was left to cool down, filtered, washed, and dried at 85 ^{0}C.

2.1.8 Calcination of the nano sized zeolite coating the 3 DOM .

The grown nano sized zeolite layer still contains the TPABr in its pores and thus blocking it. However calcination of the obtained material was taken gradually from room temperature to 350 ^{0}C at a rate of 1 ^{0}C/minute and left there for three hours and then taken to 550 ^{0}C at a rate of at a rate of 1 ^{0}C/minute and left there for two hours. This gradual calcintaion was performed in order to prevent any loss or deformation of the structure due to the burning of the polyelectrolyte layer. After this step the catalyst became ready to be evaluated in a catalytic reaction.

2.2 Characterization Techniques:

Knowledge of catalyst structure is essential to the understanding of the chemistry actually occurring in catalysis, this makes structure characterization crucial throughout the life cycle of the catalyst, from the preparation step to the use in reaction conditions.Various physical techniques were used in the characterization of the as-synthesized materials in order to understand their structural characteristics.

2.2.1 Infrared Spectroscopy:

The mid-infrared absorption region of zeolites, which contains fundamental vibrations of the framework of silica-alumina tetrahedral, can be used in the characterization of zeolite type. These vibrations include symmetric and asymmetric stretching and bending mode of Si Al tetrahedral, and double ring vibration. Jacobs et al [93] have assigned the I.R bands at 550 cm^{-1} to the vibration of the 5-member rings in ZSM-5 and the band at 450 cm^{-1} to the internal vibration of silica and alumina tetrahedral. Unique property of nanosized zeolites is a splitting of the characteristic framework vibration at 550 cm^{-1} into a doublet at 555 cm^{-1} and 570 cm^{1}. The mid infrared spectra of the as-synthesized materials was recorded on a Perkins

Elmer 61F PC spectrometer using the KBr pellets technique. About 0.5 mg of the as-synthesized catalyst sample was grinded with 500 mg of KBr in a small ball mill mortar. The mixture was transferred into a die (pellet maker) of 1 cm in diameter, and pressed for a minute at 10,000 psi under vacuum to obtain transparent pellets. The spectra was then

recorded by taking 128 scans with a resolution of 4.0 cm^{-1} and a scan range of 350 to 1400 cm^{-1}.

2.2.2 Powder X-Ray Diffraction

The crystallinity and phase purity of a synthesized zeolite can be obtained using powder X-ray diffraction (PXRD), where every crystalline material has its own characteristic XRD pattern .The powder XRD involves the use of collimated beam of X-rays , with wave length Cu K_α 0.5-2 A^0, incident on a specimen, which is diffracted by the crystalline phase in the specimen according to the well known Bragg's equation ($n\lambda=2d\sin\theta$) .The prepared powdered zeolite sample was gently grounded in an agar pestle and mortar.The fine powder was packed into a sample holder having a diameter of 1 cm and depth of 3 mm. The surface of the packed sample was smoothed with a flat glass and then powder X-ray diffraction spectra samples were recorded on a Siemens D5005 X-ray difractometer under the following operation conditions :

- Copper K X-ray radiation (λ=1.541 A^0) from a broad focus tube at 40 KV and 30mA

- Autodivergence slit with no scatter slit and a receiving slit of 0.1 mm .

- Scanning speed and interval of data collection was 0.01 degree 2θ/sec .

- Angle scanned from 0.5-50 degree 2θ .

- A graphite monochromator was used .

The nano sized zeolites that were grown on the 3DOM surface can not be characterized by the wide angle X-ray instrument mentioned above due to crystal size limitations by that instrument. However it is possible to verify the crystallinty of these nanoparticle zeolites by the use of a Transmission Electron Microscope (TEM) .

2.2.3 Thermogravimetric Analysis (TGA)

Thermogravimetric analysis (TGA) is an analytical technique used to determine a material's thermal stability and its fraction of volatile components by monitoring the weight change that occurs as a specimen is heated. The measurement is normally carried out in air or in an inert atmosphere, such as helium or nitrogen, and the weight is recorded as a function of increasing temperature. In addition to weight changes, some instruments also record the temperature difference between the specimen and one or more reference pans (differential thermal analysis, or DTA) or the heat flow into the specimen pan compared to that of the reference pan (differential scanning calorimetry, or DSC). The latter can be used to monitor the energy released or absorbed via chemical reactions during the heating process. TGA analysis of various samples was done on a Shimadzu DTG-60H apparatus. The mentioned instrument is of a vertical balance type and has two pans one is for reference (α-Alumina) and the other pan is for the sample to be analyzed. The reference crucible filled with 10 mg α-Alumina was introduced into the machine along with another empty crucible in order to calibrate the balance. After the balance is

calibrated the empty crucible is removed from the machine and filled with the sample, then introduced back to the machine and analyzed under the following conditions:

- Nitrogen gas flow

- Rate of $2^{o}C$/min up to $600\,^{o}C$.

- Weight of standard α-Alumina in the crucible ~10 mg.

- Weight of polymer used is half that of the Alumina.

2.2.4 Surface Area Measurements

Surface area is the means by which a solid interacts with its surroundings, being gas, liquid or other solids. As particle size decreases, the surface area per unit volume (or mass) increases. Furthermore, the generation of porosity, especially when due to small pores, can produce surface area far in excess of that produced by particle size reduction. On very coarse powders the specific surface area can be as low as a few square centimeters per gram, while on finer powders it might be a few square meters per gram. Porous materials having a significant volume of very small pores might exhibit a surface area larger than a football field - several hundreds square meters per gram. Surface area measurement is probably the most widely used means to characterize porous materials. Since the surface area corresponds to the roughness of the particle exterior and its porous interior, gas sorption is the preferred technique. Generally the temperature and pressure of an inert gas are adjusted to cause a single layer of gas molecules to be adsorbed over the

entire surface of a solid, be it porous, non-porous or powdered. Pressure transducers or other sensors respond quantitatively to the amount of gas adsorbed. Using these data, and by means of a simple well-known calculation (the B.E.T. equation), it is easy to compute the surface area of a sample which is usually reported as the *specific* surface area or surface area per unit mass, usually m^2/g. Surface area of the as synthesized 3DOM carbon, and 3DOM carbon with nano-sized zeolites grown on the surface both before and after calcination were recorded on a NOVA-2200 Ver. 4.01.

2.2.5 Scanning Electron Microscope (SEM)

Electron microscope is used to study the crystal morphology and size of the particles. In SEM an electron beam is focused into a fine probe and subsequently scanned over a small rectangular area. As the beam interacts with the sample it creates various signals, all of which can be appropriately detected. These signals are highly localized to the area directly under the beam. By using these signals to modulate the brightness of a cathode ray tube, which is scanned in synchronism with the electron beam, an image is formed on the screen. This image is highly magnified and usually has the look of a traditional microscopic image but with much greater depth of field.

A small amount of the catalyst sample was mounted on a copper holder. The sample was coated with gold evaporated under high vacuum. The SEM equipment used was a Joel JSM-500. Micrographs were taken for samples of the latex spheres, 3DOM carbon, and 3DOM carbon with grown zeolites on the surface before and after calcination at different magnifications ranging from 15000 to 100000 times.

2.2.6 ^{27Al} and ^{29}Si solid state NMR

Solid state NMR, generally employing magic angle sample spinning (MAS), is a technique for providing information on the molecular structure and dynamics of the atoms present in a certain framework. Alumina can exist in the framework in a tetrahedral coordination or as an extra-framework in an octahedral coordination, both of these species can be identified by NMR .The presence of tetrahedrally coordinated alumina is taken as an indication of a zeolitic material. In a zeolite framework the more alumina is in the tetrahedral fashion the more crystalline it is whereas the octahedral fashion reflects amorphous alumina. Whereas for Silica the more Q_4 and Q_3 peaks the more crystalline the zeolite is because Q_4 represents silica in the tetrahedral fashion while Q_3 represents tetrahedral silica bonded to an alumina. The samples were grinded into fine powder in a zirconia probe and sealed well before running the spectrum on a Joel JNM - LA 500 FT NMR system.

2.2.7 Elemental Analysis / Inductively Coupled Plasma

In Inductively Coupled Plasma Atomic Emission Spectroscopy (ICP-AES), a gaseous, or liquid (as an aerosol) sample is injected into the center of a gaseous plasma .The sample is vaporized, atomized, and partially ionized in the plasma. Atoms and ions are excited and emit light at characteristic wave-lengths in the ultraviolet or visible region of the spectrum. The emission line intensities are proportional to the concentration of each element in the sample. A grating spectrometer is used for either simultaneous or

sequential multi elemental analysis. The concentration of each element is determined from measured intensities via calibration with standards.

Sample preparation for the catalyst was done by calcining the prepared catalyst in air in order to burn out the carbon while retaining the nanosized zeolites that are grown on the walls. A 100 mg of dried zeolite was weighed in a 10 ml platinum crucible and mixed with 300 mg of lithium metaborate. The crucible was kept in a muffle furnace at 950 ^{o}C for 30 minutes. When a clear melt was obtained, it was cooled down and the melt was agitated in 5% hydrochloric acid with gentle warming. When completely dissolved it was transferred to a 100 ml volumetric flask and diluted with distilled, deionized water to the final volume.This solution was used for the determination of the major elements (Si,Al) in the zeolite nanoparticles .The instrument used for chemical analysis of the synthesized zeolite samples was a Spectro Ciros Vision ADS 500.

2.2.8 Catalyst Evaluation:

2.2.8.1 Reaction Apparatus and Parameters:

The experimental setup used in the evaluation of catalyst consists of a feed system containing n-hexane(99.67% purity) ,carrier gas system containing high purity argon gas as the feed carrier, tubular stainless steel reactor, an outlet exhaust, temperature controller system, and a bubbler system used to introduce n-hexane into the reactor operating at 0 ^{o}C to ensure a constant partial pressure of n-hexane (6.0KPa) at atmospheric pressure. The

reactor is 21cm long stainless tube with an internal diameter of about 1cm. Diagram of the experimental set up is shown in figure 2.2.

The feed consists of 6.0 kPa partial pressure n-hexane at 0 ^{o}C, and 95.3 KPa argon (99.99% purity). The catalytic reactions were carried out over about 0.435 gr of the catalyst under atmospheric pressure and temperature range from 300 ^{o}C to 380 ^{o}C. The flow rate was varied from 9 ml/min to 18 ml/min.

2.2.8.2 Catalytic Test :

The catalytic activity of the synthesized materials in n-hexane cracking between 300 and 380°C was investigated using a fixed bed micro-reactor system operating at atmospheric pressure. In all catalytic runs, about 0.435 gr of the synthesized catalyst was used. The catalyst was sandwiched between the quartz wool at the isothermal region of the reactor, and the remaining part was filled with inert aluminum granules. A flow of nitrogen gas was passed through the reactor for six hours in order to activate the catalyst, then argon gas at a predetermined rate was bubbled through an n-hexane saturator at 0 ^{o}C into the reactor. The reactor effluent was collected in a gas tight syringe every 20 minutes and analyzed using a gas chromatograph equipped with a flame ionization detector and potassium iodide alumina plot column. From the GC results, the n-hexane fractional conversion (x) was obtained and the rate constant (k) was obtained from the slope of the first order plot of -Ln(1-x) against contact time at a given reaction temperature. The activation energy *E,* was calculated from an Arhenius plot of Ln k against T $^{-1}$. The

absence of thermal cracking was confirmed with blank experiment using 3 DOM carbon only in place of the catalyst.

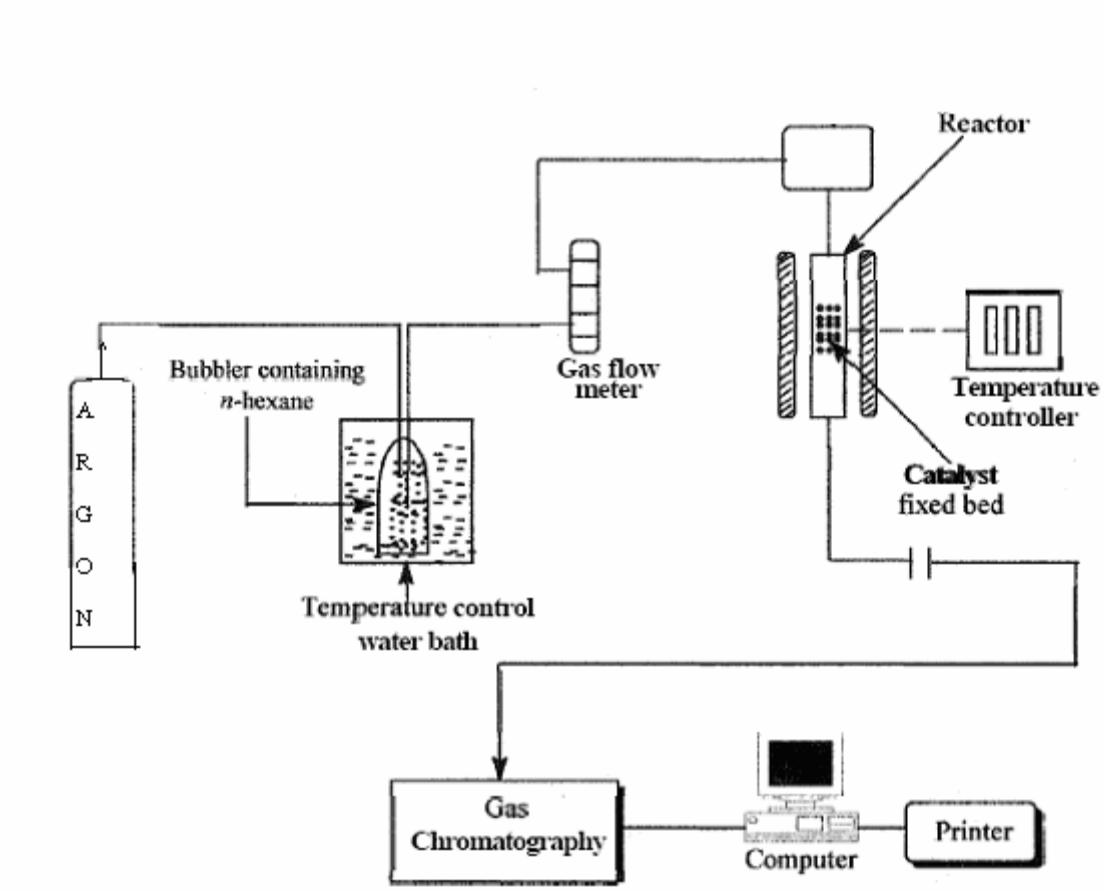

Figure 2.2 : Schematic representation of the experimental setup for the n-hexane cracking reaction .

2.2.9 Complete degradative reaction of high density polyethylene with powdered zeolites and zeolite coated carbon catalyst.

The complete degradative reaction of polyethylene and powdered zeolites from one side and the prepared catalyst from another side took place in a quartz tube reactor connected to an external product collector. Samples of polyethylene and powdered zeolites or carbon supported zeolite were introduced into a quartz tube reactor and heated at 100 ^{o}C for an hour over flowing nitrogen gas in order to get rid of the moisture filling the pores .After that the collector was immersed in an ice bath, nitrogen flow was stopped, and the temperature was increased to 350 ^{o}C within 2 minutes .Gaseous products were collected from a hose placed 2cm from the bottom of the collector while liquid products were left in the collector tube. Gaseous products were analyzed by GC in order to determine the composition and weight percentage of each component, while the liquid products were analyzed by Gel Permeation Chromatography in order to determine the molecular weight distribution of its components .

CH: 3

Results and Discussion

3.1 Synthesis and structural analysis of the catalyst

3.1.1 Analysis of colloidal crystal template tynthesis :

All attempts to synthesize the catalyst requires the preparation of a colloidal crystal template from a non-crosslinked poly(methyl methacrylate) monodisperse latex dispersion, which can be synthesized using an emulsifier-free emulsion polymerization technique. As a result monodisperse latex spheres suspended in solution are formed. Before use; the spheres are closed-packed into colloidal crystals as shown in Figure 3.1 by either gravity sedimentation or centrifugation followed by drying at room temperature.

3.1.2 Analysis of 3 DOM synthesis:

The next step which is also common for all attempts is the preparation of a 3 DOM carbon which is done by saturating the latex with a resorcinol formaldehyde solution catalyzed by sodium carbonate. The latex resorcinol composite is filtered, dried and later calcined to carboryze the carbon and to remove of the latex leaving behind a 3 DOM structure as shown in Figure 3.2.

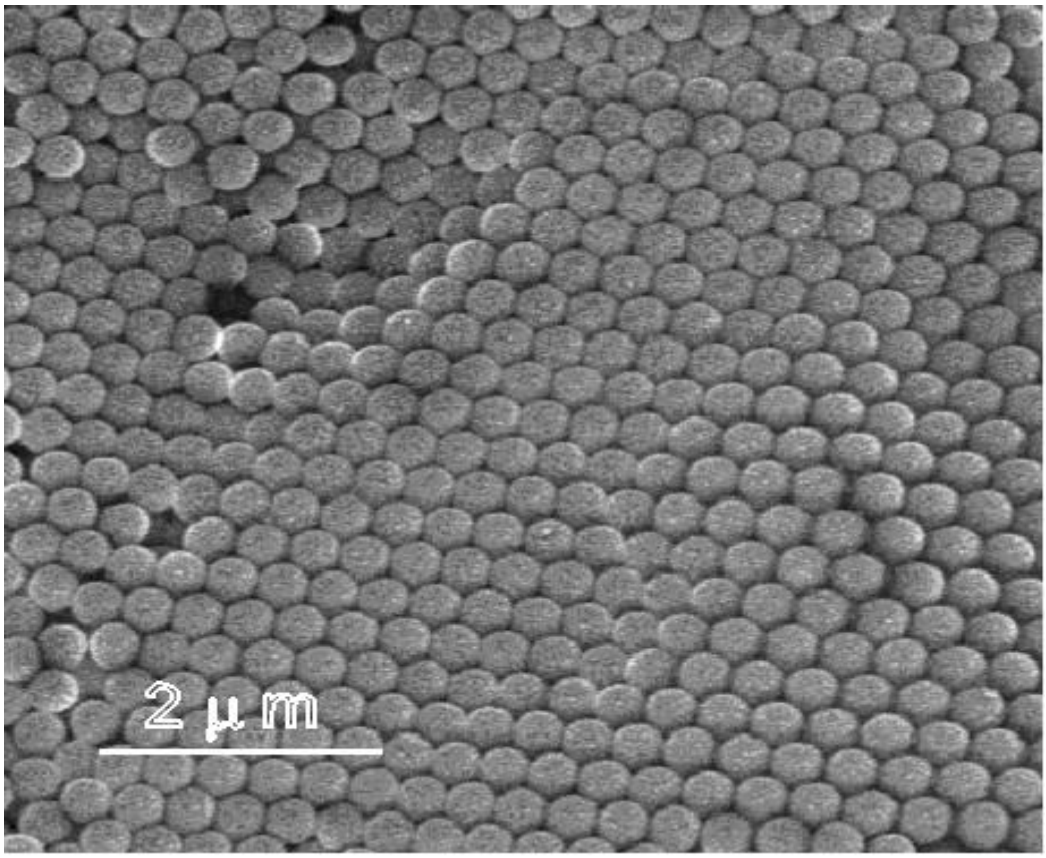

Figure 3.1: SEM image of close-packed colloidal latex spheres.

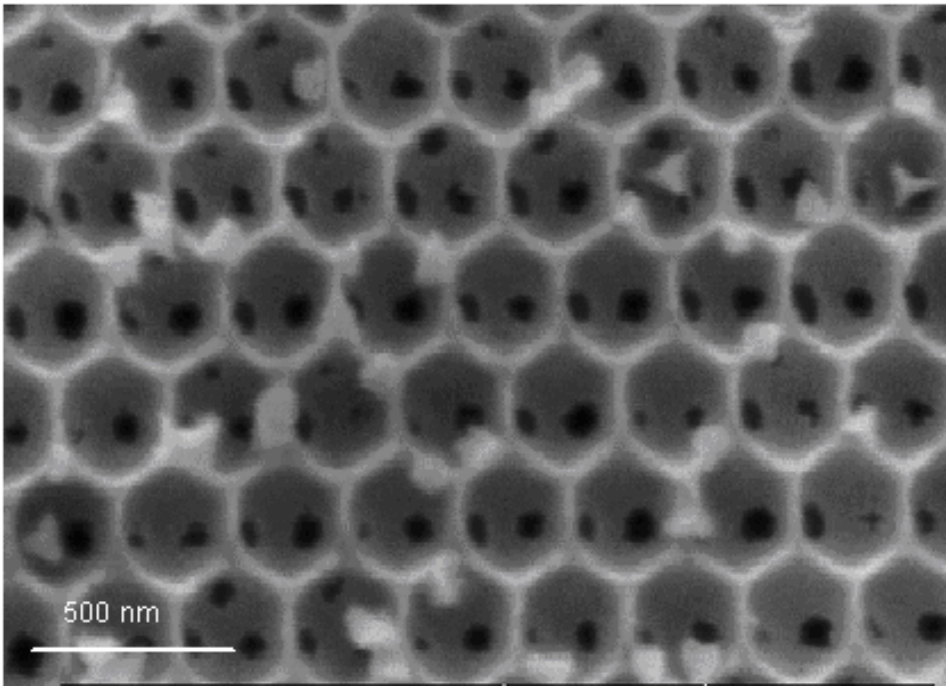

Figure 3.2: SEM image of 3 DOM carbon.

3.1.3 Titration results of the 3 DOM carbon

The prepared 3 DOM carbon was titrated according to the procedure described in 2.1.3 in order to determine the pH at which the surface charge of the carbon is zero. The point of zero charge was obtained after plotting the volume of acid and base versus the pH of the

three salt solutions with different ionic strengths as shown in Table 3.1. The point of intersection of the three curves as shown in Figure 3.3 is the point at which the surface charge of carbon is zero and as shown in the figure that point occurred at a pH of 4.

3.1.4 Polyelectrolyte coating of the 3 DOM structure

After the 3 DOM was titrated and the point of zero charge was found to be at a pH of 4 then if the carbon is dispersed in a solution of pH 4 and above it will hold a negative charge on its surface .Since the zeolite precursor solution have a pH of around 8 which indicate that the zeolites are negatively charged, their growth on a negatively charged carbon surface will not take place due to charge mismatching. Therefore the interface between the carbon and zeolite must provide favorable charge interaction and that was achieved by coating the carbon with a polyelectrolyte multilayer starting with the first layer as positive and ending with the last layer as positive also as shown by the schematic sketch in Figure 3.4 .

	pH of 45 ml 0.1 M KNO_3 + 0.15 g carbon	pH of 45 ml 0.01 M KNO_3+ 0.15 g carbon	pH of 45 ml 0.001 M KNO_3+ 0.15 g carbon
1.5 ml KOH	12.17	12.16	12.03
1.0 ml KOH	11.95	11.96	11.63
0.5 ml KOH	11.37	11.48	10.38
0.25 ml KOH	9.78	8.4	7.48
0 ml	5.37	5.34	5.08
0.25 ml HNO_3	3.07	2.99	2.87
0.5 ml HNO_3	2.65	2.66	2.5
1.0 ml HNO_3	2.35	2.32	2.16
1.5 ml HNO_3	2.15	2.09	1.96

Table 3.1: pH values of the three salt solutions.

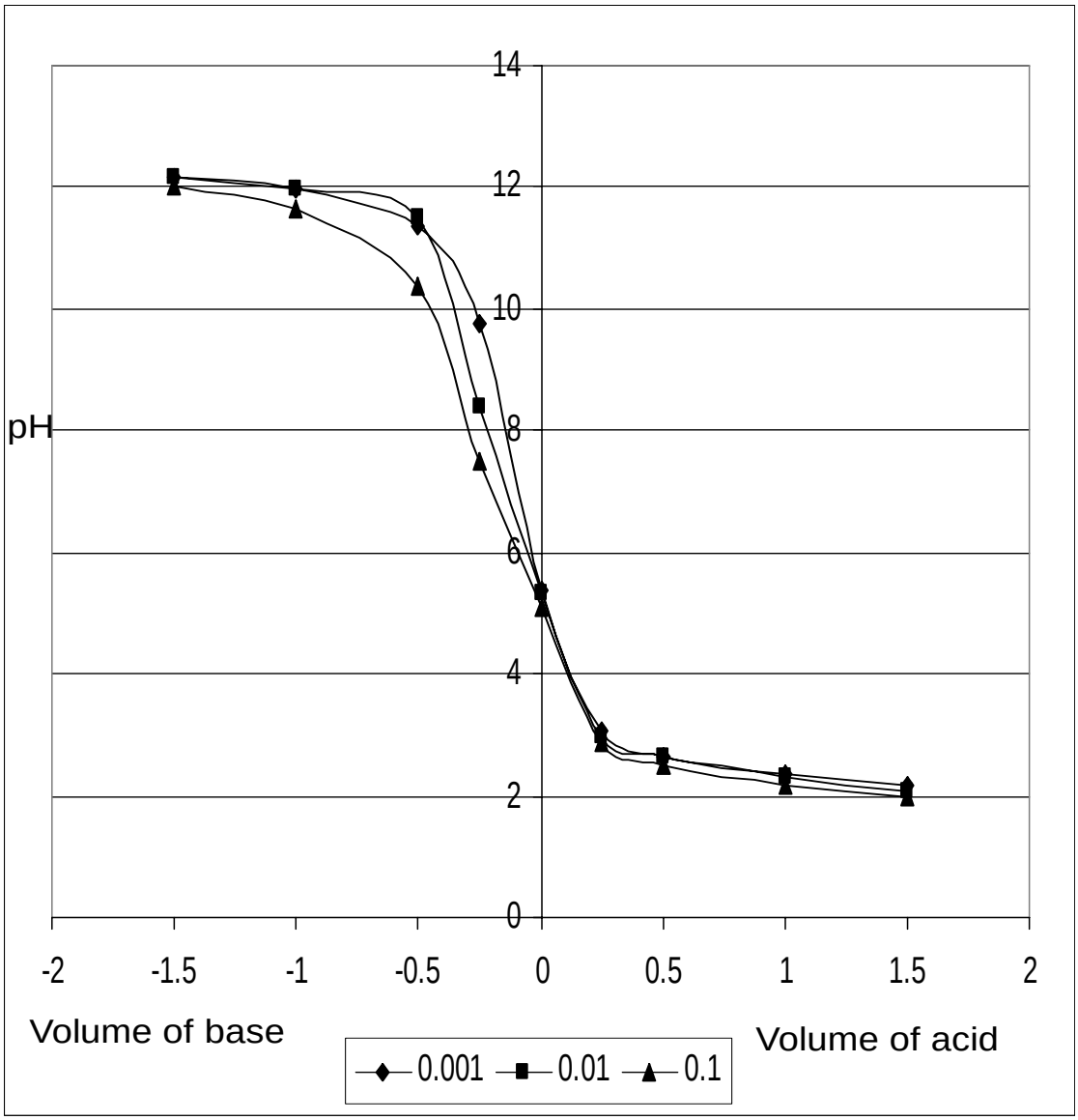

Figure 3.3: Plot of pH versus volume of the acid and base.

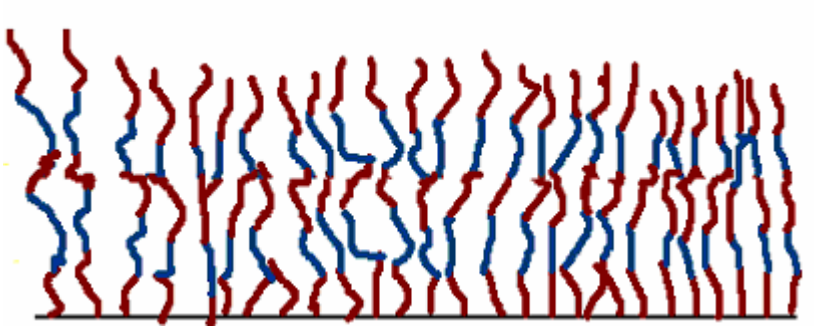

Figure 3.4: Schematic sketch of a polyelectrolyte multilayer grown on a carbon surface.

3.1.5 Analysis and results of zeolite growth on 3 DOM surface

The first synthesized catalyst was prepared according to the procedure described in section 2.1.6 but the 3 DOM carbon used was not modified with a polyelectrolyte multilayer and as a result zeolites did not grow on the walls of the 3 DOM. Instead crystallization took place in solution and the zeolite crystals deposited on the surface of the 3DOM as shown in Figure 3.5 in the form of clusters which are aggregates of zeolite nano particles. The obtained result was expected to be so because the surface charges on both carbon and zeolites didn't match and thus zeolite growth took place in the solution and deposited as clusters on the outer surface rather than grow on the walls of the 3DOM .

The second catalyst was prepared in the same way as the first one but the 3 DOM carbon used was modified with a polyelectrolyte multilayer composed of commercial positive poly diallyl dimethyl ammonium chloride 20 % solution in water as shown in Figure 3.6 and negative poly sodium 4-styrene-sulfonate 30% solution in water as shown in Figure 3.7. In this case the zeolite was found to grow on the walls of the 3 DOM partially as shown in Figure 3.8 and was not uniform in addition to deposition of large clusters on the external surface like those observed in the first catalyst. The reason for such a result is that the first layer in the polyelectrolyte multilayer system in contact with the carbon is the positive poly diallyl dimethyl ammonium chloride with a surface charge density greater than that of the carbon surface and thus coating was not uniform on the carbon surface.

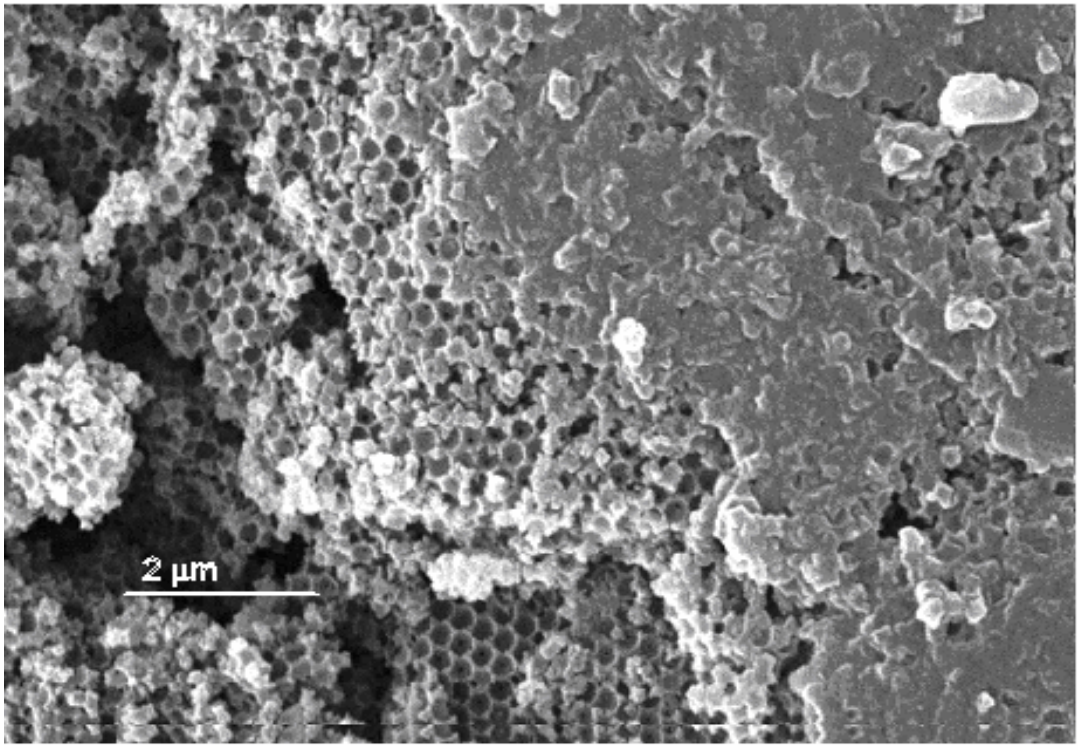

Figure 3.5: SEM of the first catalyst

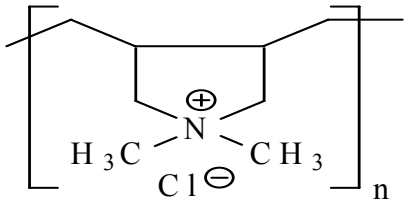

Figure 3.6 : Structure of positive poly diallyl dimethyl ammonium chloride 20 %

solution in water .

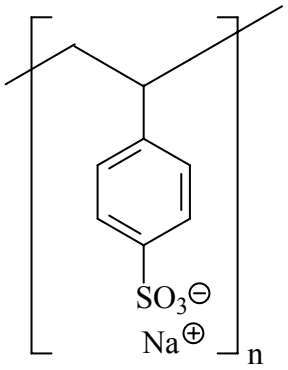

Figure 3.7 : Structure of negative poly sodium 4-styrene-sulfonate 30% solution in water .

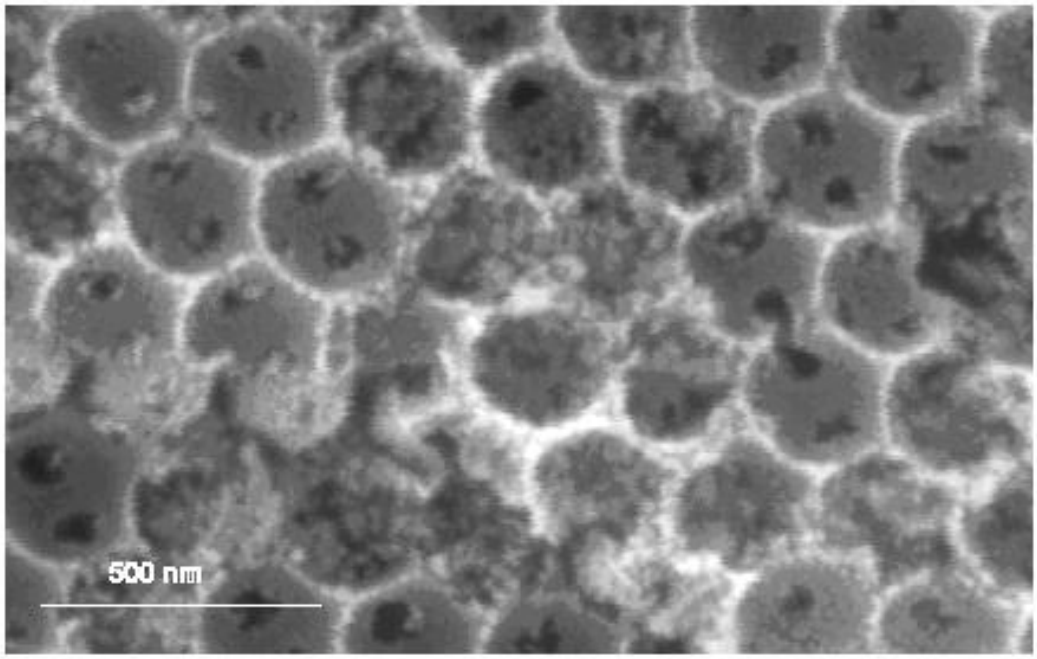

Figure 3.8: SEM of the second catalyst.

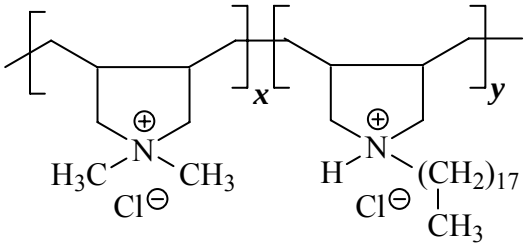

Figure 3.9: Structure of modified positive polymer with x= 96% and y = 4 %.

The third catalyst was prepared with an attempt to avoid the surface charge density mismatching between the carbon and the first positive polyelectrolyte layer. In this case a different positive polyelectrolyte another positive polyelectrolyte as shown in Figure 3.9 was used for first layer coating .As it is noticed this new positive polymer have around 4% hydrophobic C_{18} chains in its backbone, and due to the presence of these hydrophobic tails , the surface charge of the polymer was altered and became close to that of carbon. This way the hydrophobic tail interacts more favorably with the hydrophobic carbon surface than the commercial positive polymer that we used in the synthesis of the second catalyst .As a result of this modification and surface charge matching, the zeolites were grown on the walls of the 3 DOM carbon in a uniform fashion as shown in Figures 3.10a and 3.10b .

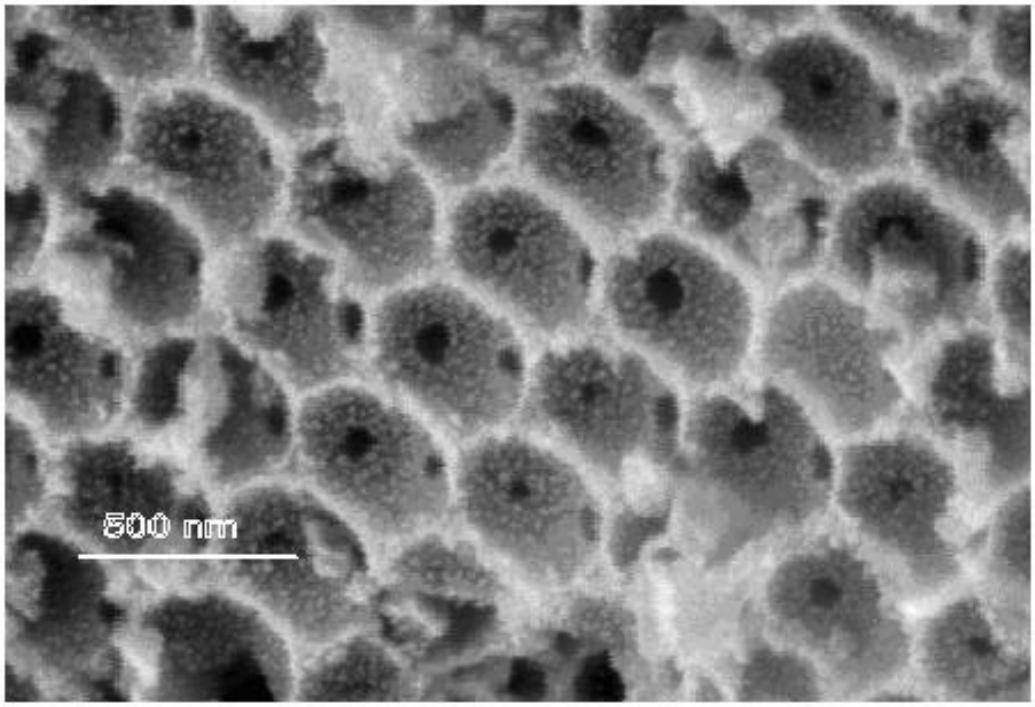

3.10a : SEM image of the third catalyst (low magnification).

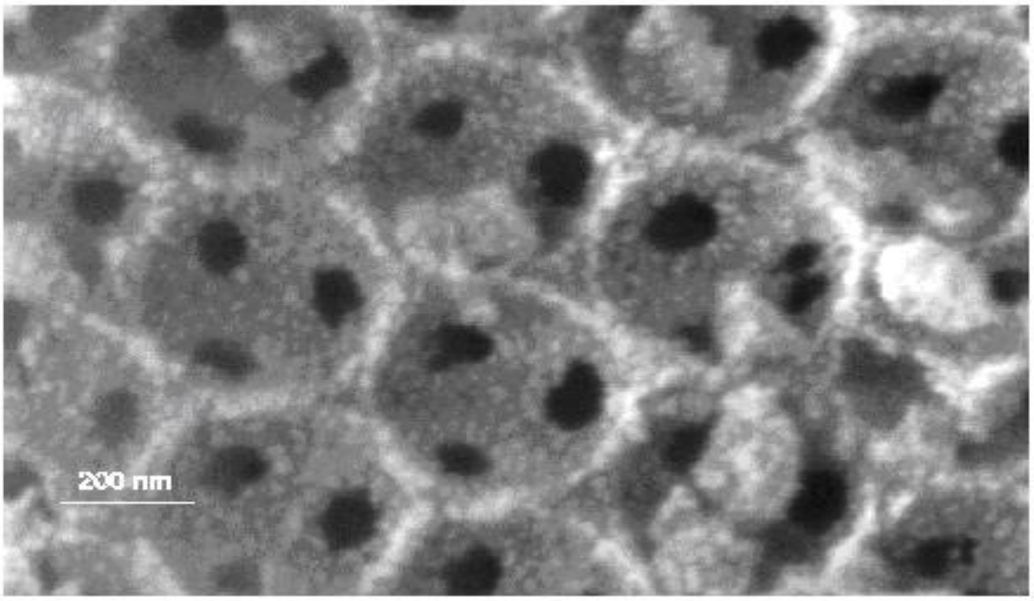

3.10b : SEM image of the third catalyst (high magnification).

3.2 Infrared spectral analysis of the synthesized material

The mid-IR region (1400cm^{-1}-300cm^{-1}) is useful for zeolite characterization since it contains the fundamental vibrations of the framework silica-alumina tetrahedral. A typical spectrum of well crystallized ZSM-5 zeolite (Figure 3.11a) contains absorption band at 1100, 800 and 450 cm^{-1}, which coincide with that of silica alumina (Figure 3.11b) and have been assigned to the asymmetric stretching and bending modes of the $Si(Al)O_4$ tetrahedral respectively. In addition, distinct absorption bands that are structural sensitive are observed at 1225$cm^{-1}$and 550 cm^{-1}, as reported by Jansen et al [94]. These two bands, observed in zeolite with five member rings, are of vital importance as they help in differentiating zeolite type.

The first structure sensitive band at 1225cm^{-1} due to external asymmetric stretching vibration is clearly present in IR spectra of ZSM-5 zeolite with four chains of five member rings arranged around two-fold screw axis of the zeolite framework and it also appeared strongly in the IR spectrum of the zeolite coated carbon catalyst as shown in figure 3.11c. According to Jacobs et al [95], the second structure sensitive absorption band at 550 cm^{-1} is due to the vibration of the 5-member rings in ZSM-5 and the band at 450 cm^{-1} to the internal vibration of silica and alumina tetrahedral. However unique property of nanosized zeolites is a splitting of the characteristic framework vibration at 550cm^{-1} into a doublet at 555cm^{-1} and 570cm^{1}.These absorption peaks appeared with strong intensity in the spectrum of the third catalyst as shown in Figure 3.11c, thus verifying the growth of nano-sized MFI type aluminosilicate zeolite .

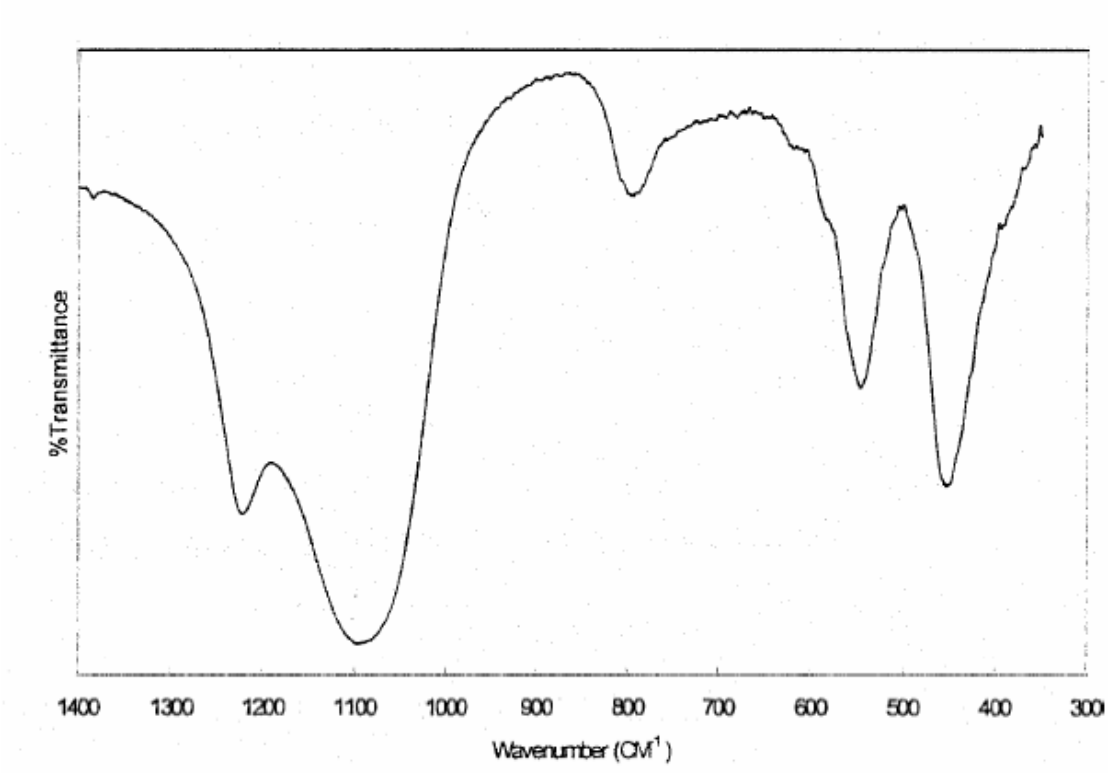

Figure 3.11a: A typical IR spectrum of the framework region (1400-300cm^{-1}) of ZSM-5

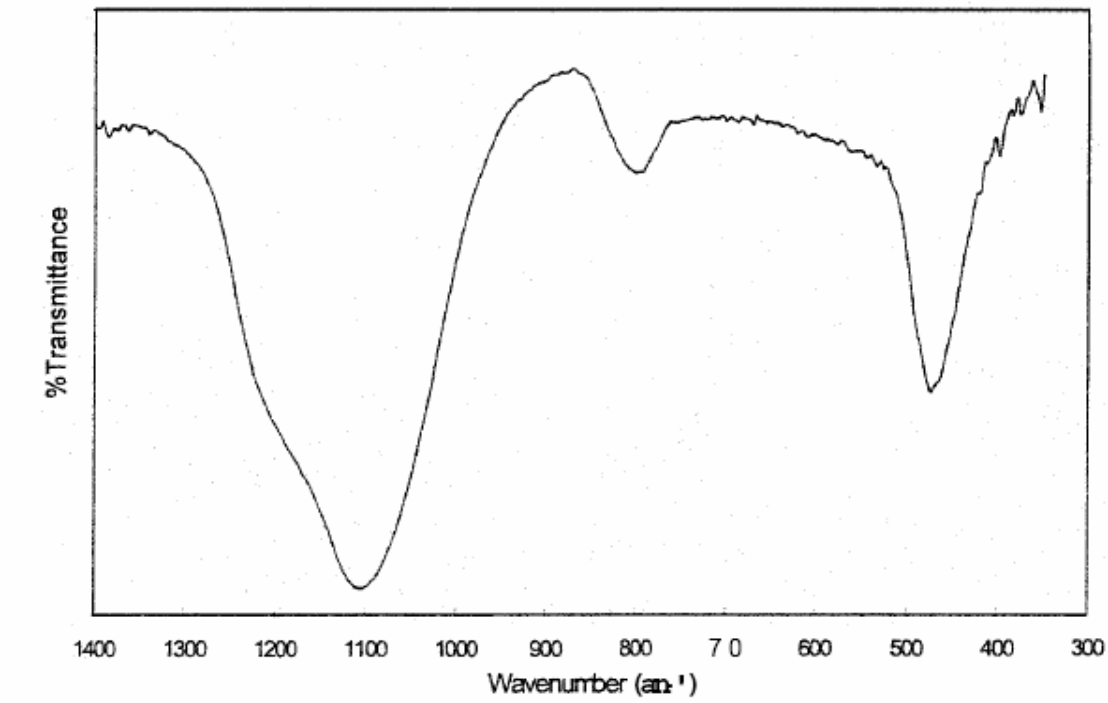

Figure 3.11b: A typical IR spectra of the framework region (1400-300cm^{-1}) of Silica alumina

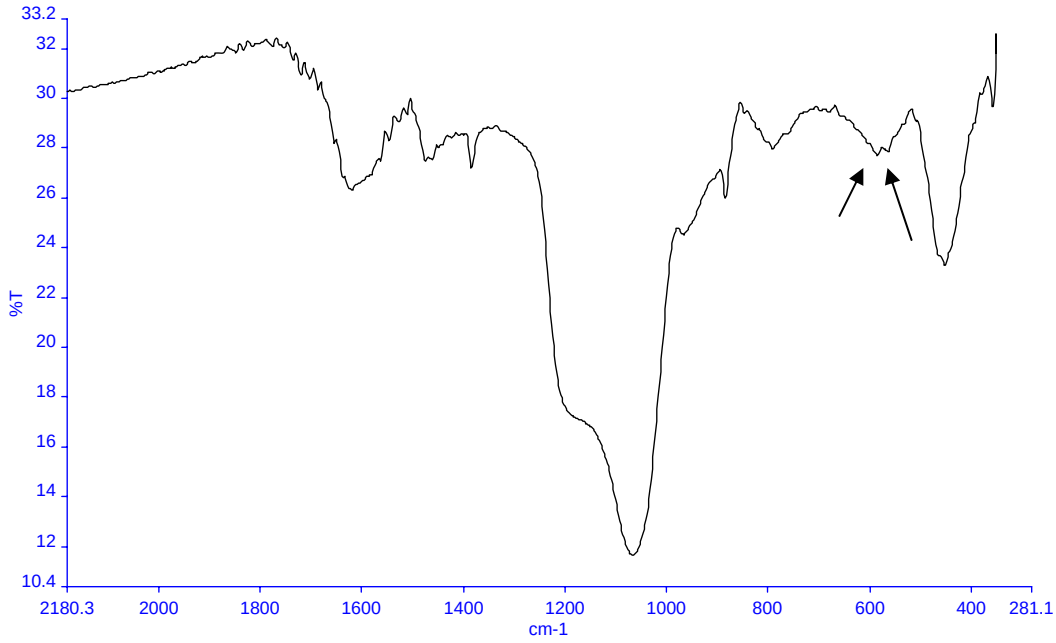

Figure 3.11c: Framework IR spectra of the as synthesized catalyst.The arrowheads indicate the splitting of the band into a doublet (555 and 570 cm-1) in silicalite nanoparticles .

3.3 X-Ray spectral analysis of the synthesized material

Zeolites being crystalline solids with a regular structure have a characteristic diffraction pattern; this can be used to identify the material and determine the degree of crystallinity. Powdered zeolites were prepared in order to compare the activity of the zeolite carbon coated catalyst to that of powdered zeolites. The powder x-ray diffraction pattern of the as-synthesized powdered zeolite is shown in Figure 3.12a and the calcined sample in Figure 3.12b. The diffraction pattern is characteristic of the MFI structure, shown in Figure 3.12c, thus verifying that the prepared powdered zeolite is of an MFI type. However the crystallinity of nanosized zeolites that were grown on the walls of the 3 DOM carbon can not be verified by wide angle X- ray diffraction instrument and thus an alternative instrument such as TEM can verify this property.

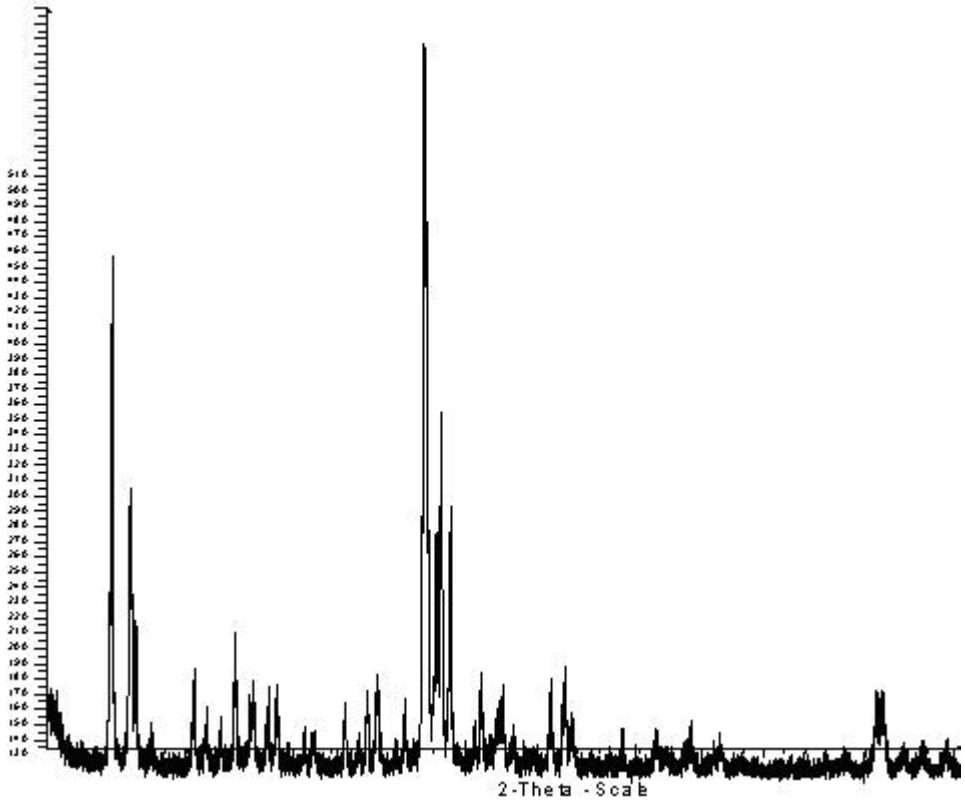

Figure 3.12a : Powder X-ray diffraction pattern of the as synthesized powdered zeolite .

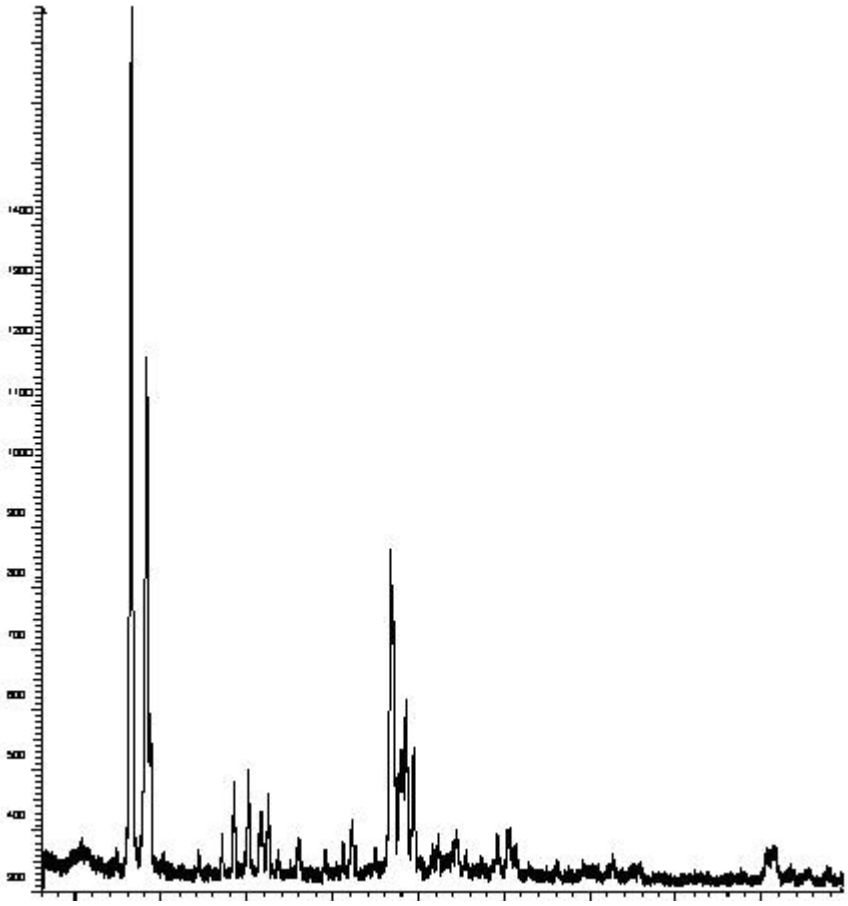

Figure 3.12b : Powder X-ray diffraction pattern of the calcined powdered zeolite .

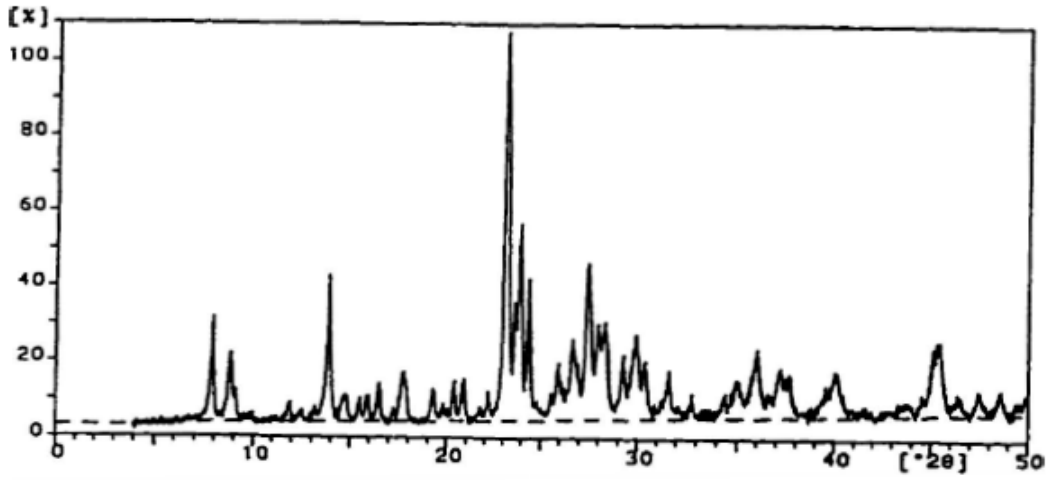

Figure 3.12c : Powder X-ray diffraction pattern of standard ZSM-5 .

3.4 Thermo Gravimetric Analysis (TGA) results

Thermal analysis carried out in air reveals information concerning the amount of zeolites loaded on the walls of the 3 DOM as shown in the TGA – DTA curve in Figure 3.13a where the amount of zeolite loading in the 3 DOM framework was determined to be 41.7

% .In addition to that TGA for the as-synthesized zeolite coated catalyst under nitrogen shown in Figure 3.13b was done in order to study the thermal stability of the catalyst and the temperature at which the polyelectrolyte burns. As it can be noticed that the weight loss after thermal analysis in air took place completely at 600 ^{o}C whereas in nitrogen there was no change in weight at 600 ^{o}C .

3.5 Surface area measurement analysis

Specific surface area for 3DOM carbon alone, powdered zeolite, and for the as synthesized zeolite coated catalyst before and after calcination was measured by nitrogen adsorption at liquid nitrogen temperature using the BET method. The measured specific surface area of the as-synthesized 3 DOM carbon was found to be 569.2 m^2/g, such a high surface area is obvious due to the micro porosity of the 3DOM framework. As expected the measured specific surface area of the as-synthesized catalyst before calcination was found to be 573.24 m^2/g which is almost the same as that of 3DOM carbon alone and that is because before calcination the grown zeolites are like a layer coating the 3DOM and thus not contributing anything to the framework porosity. However after calcination of the as-synthesized catalyst the micro pores of the zeolite nanoparticles on the 3DOM walls are opened after the removal of the alkyl ammonium template, which led to an obvious increase of the measured specific surface area to reach 672.6 m^2/g. The measured specific surface area of calcined powdered zeolite was 361.75 m^2/g which is similar to that of commercial powdered zeolites.

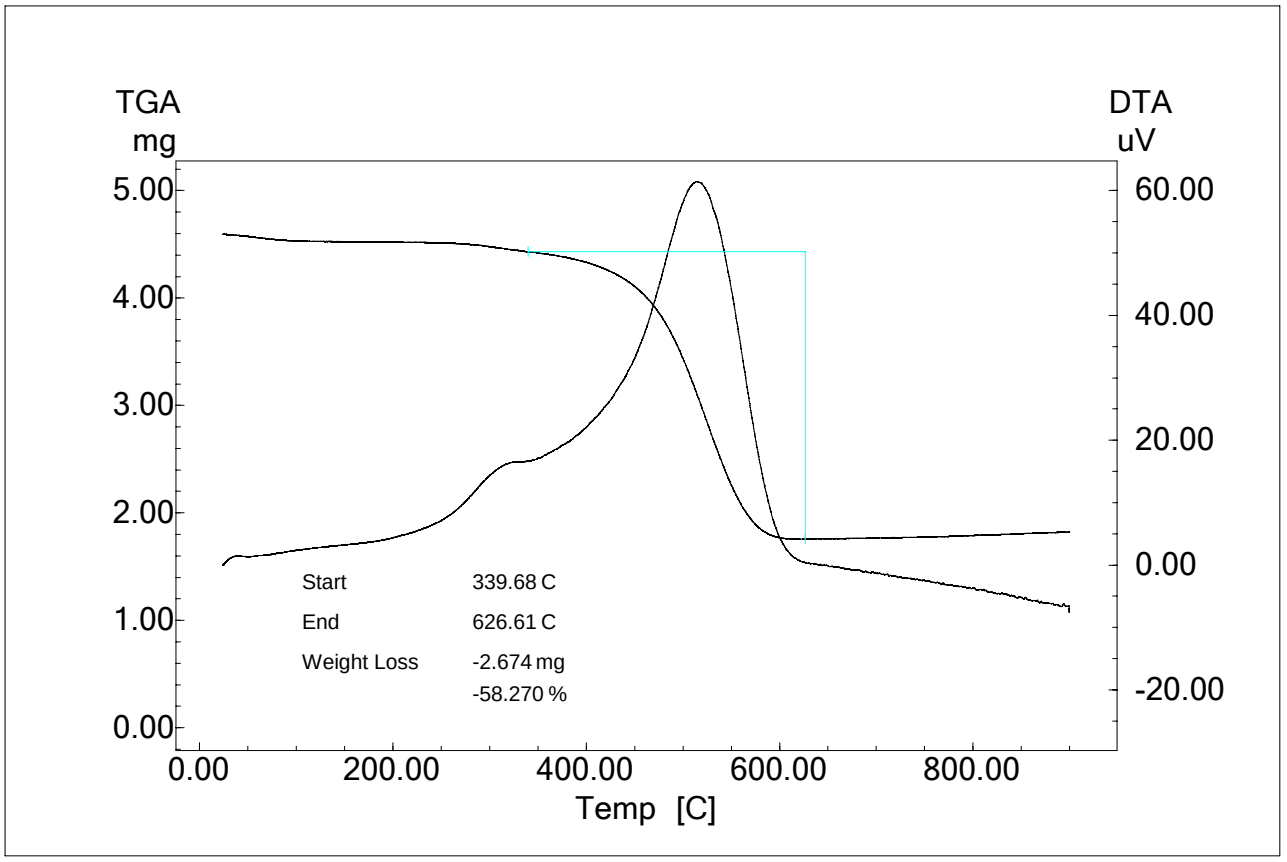

Figure 3.13a: TGA-DTA curve for the as-synthesized zeolite coated catalyst in air.

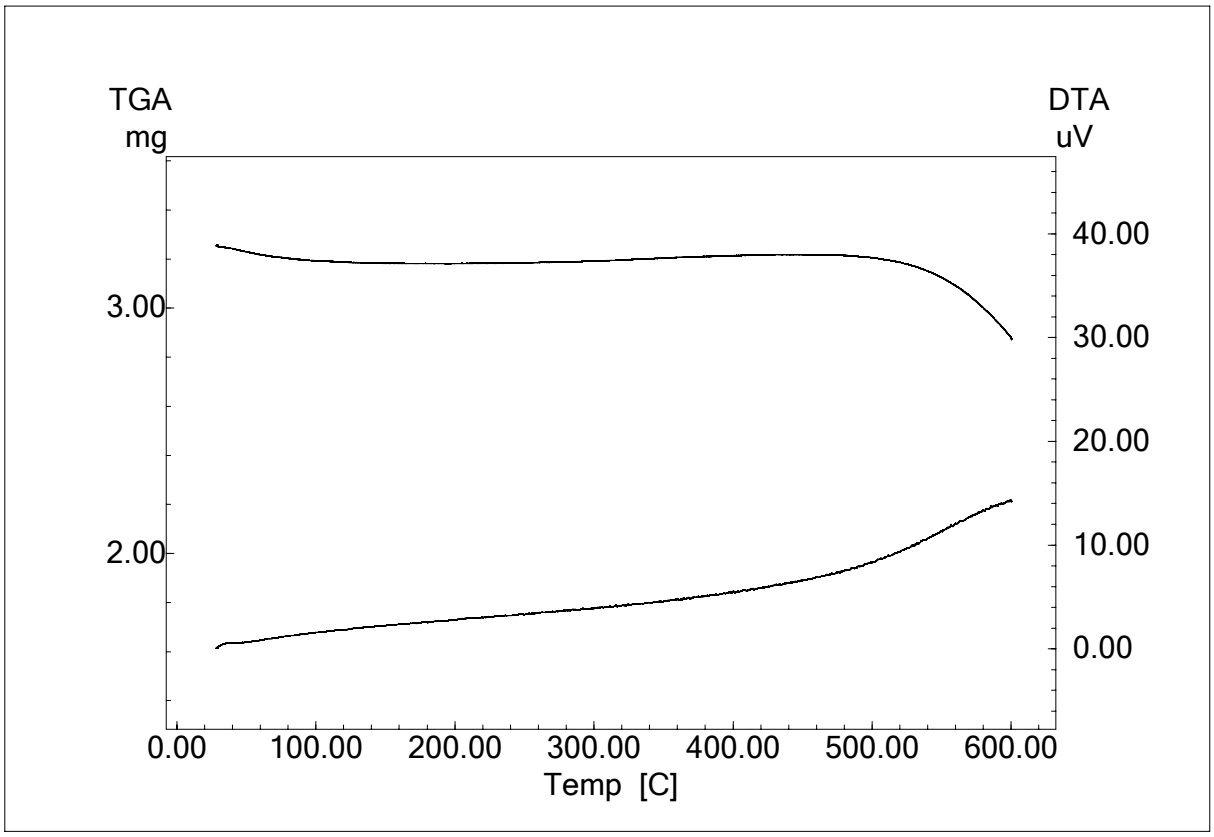

Figure 3.13b: TGA-DTA curve for the as-synthesized zeolite coated catalyst in N_2 .

3.6 ICP analysis results

The initial zeolite precursor composition used in the synthesis of the catalyst had a starting Si/Al ratio of 58; however not all of the zeolite precursor was turned into zeolite nano particles on the 3DOM walls. Also many reaction parameters such as alkalinity, water content, stirring rate, and duration of crystallization affects the ratio of silica to alumina in the zeolite nano particles. That was revealed by the results of the ICP-AS elemental analysis where the Si/Al ratio was found to be around 12.

3.7 ^{27}Al and ^{29}Si solid state NMR

Silica and alumina NMR is a useful technique for providing information on the molecular structure and dynamics of the atoms present in a certain framework.

^{29}Si NMR spectra of the zeolite coated carbon catalyst before and after calcination is shown in Figures 3.14a and 3.14b respectively. As it can be noticed that before calcination the intensity of Q_3 and Q_4 peaks are higher than that of Q_1 and Q_2, and that reflects the order and crystallinity since we have more silica in the tetrahedral fashion. However in the calcined sample the intensity of Q_4 and Q_3 relative to Q_1 and Q_2 increased a little due to some deformation in the structure as the polyelectrolyte and TPABr were burned. Also from the spectra Si to Al ratio can be obtained and it was found to be 6.08 before and 6.25 for the calcined and uncalcined sample respectively.

^{27}Al NMR spectra of the zeolite coated carbon catalyst before and after calcination exhibited two resonance peaks as shown in figure 3.14c at chemical shifts of 0 (reference

octahedral) and -51 (tetrahedral) ppm. Before calcination the octahedral and tetrahedral peaks had intensities of 0.71 and 1 respectively which meant that around 60 % of the alumina is in tetrahedral framework implying that the crystallinty of the zeoliteon the carbon is 60%, whereas in the calcined sample the intensities of octahedral and tetrahedral peaks were 1.18 and 1 respectively which meant that the amount of octahedral aluminum increased and that was also observed in the Si /Al ratio from ^{29}Si NMR.

After calcination approximately 50% of total aluminum existed in an octahedral state since from the ^{27}Al NMR spectra of the calcined sample the ratio of Al_{td}/Al_{Oh} is almost 1 in addition to that the Si/Al ratio from ^{29}Si NMR is around 6.25 which is approximately half of that given by ICP.

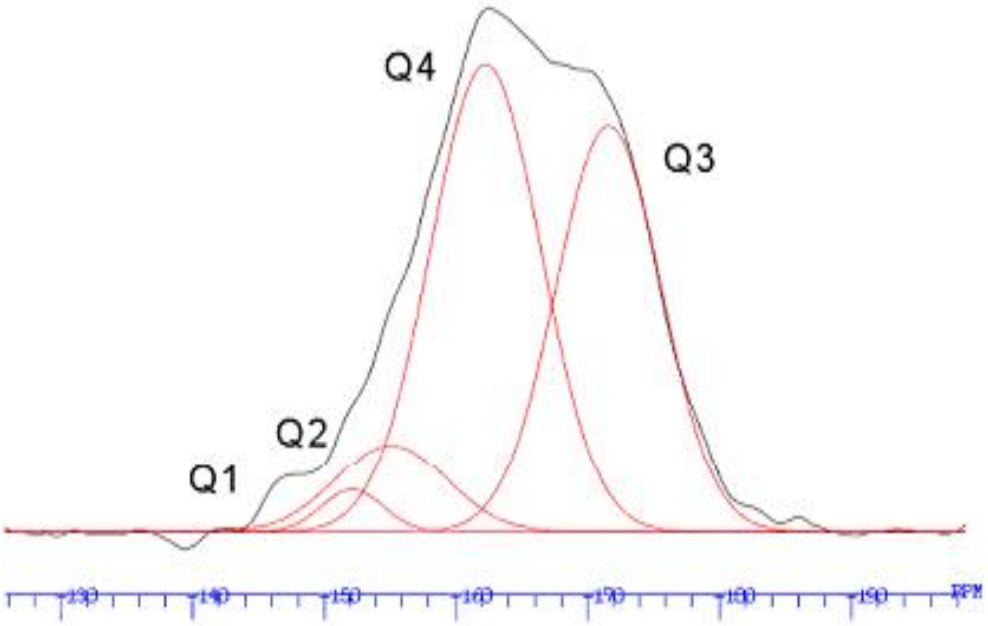

Figure 3.14a: ^{29}Si NMR spectra of as-synthesized zeolite coated carbon catalyst before calcination .

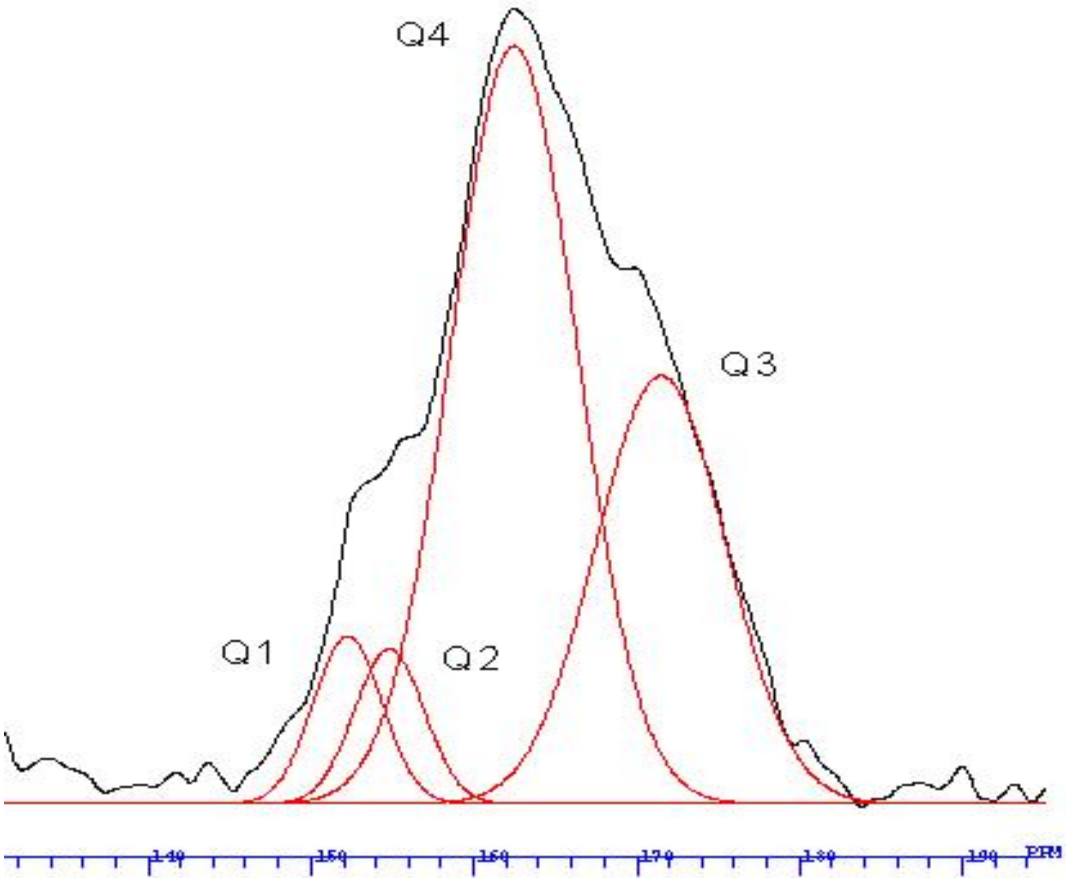

Figure 3.14b: ^{29}Si NMR spectra of the zeolite coated carbon catalyst after calcination

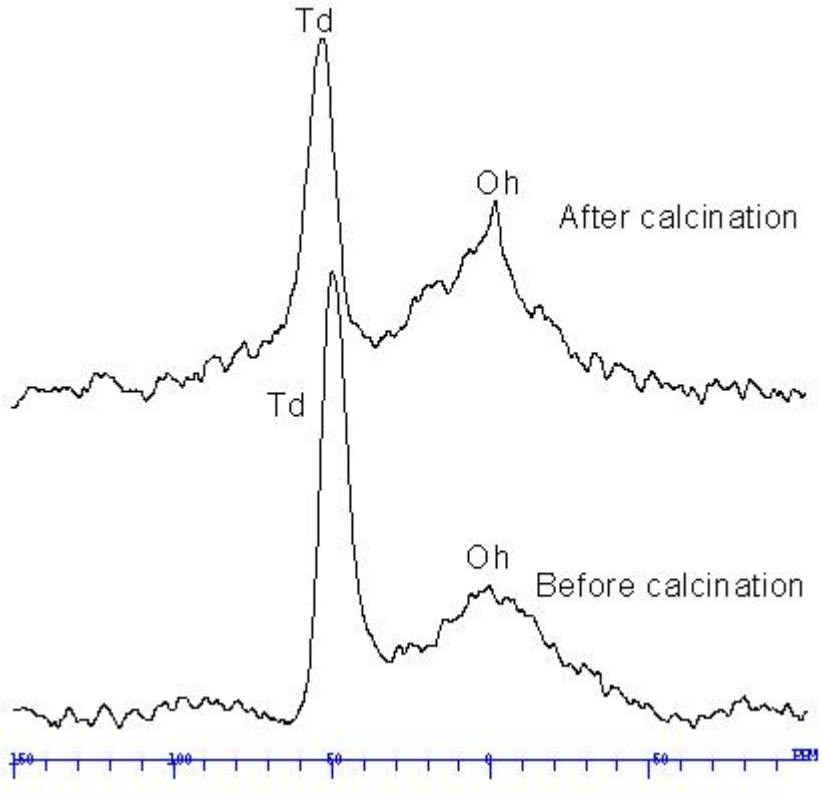

Figure 3.14c: ^{27}Al NMR spectra of as-synthesized catalyst before and after calcination .

3.8 Catalyst activity(acidity) by n-hexane cracking

It is well known that the modul compound cracking kinetic is first order in n-hexane and the curve of- ln(1- x) in which x is the fractional conversion (%) of n-hexane, as a function of the contact time is expected to be linear. Thus the apparent rate constant can be calculated from the first order rate equation Ln(1 - x) =-KT , where T is the space time defined by the flow rate divided by the volume of the catalyst. The plot of - In(1- x) Vs space time of the catalyst at three different temperatures is provided in Figure 3.15.

Generally, a linear increase of - ln (1- x) when the contact time increases was observed even at the lower temperature 300°C. This proves that the n-hexane cracking reaction over the catalyst tested follows a first order kinetics. For each temperature, the values of rate constant (k) obtained from the slope of the first order plot of - ln(1- x) against space time at that given temperature is shown in Table 3.1 .

Temperature (^{o}C)	Rate constant k (min^{-1})
300 ^{o}C	0.0449
340 ^{o}C	0.0939
380 ^{o}C	0.1484

Table 3.2 : Rate constants of n-hexane cracking at different temperatures

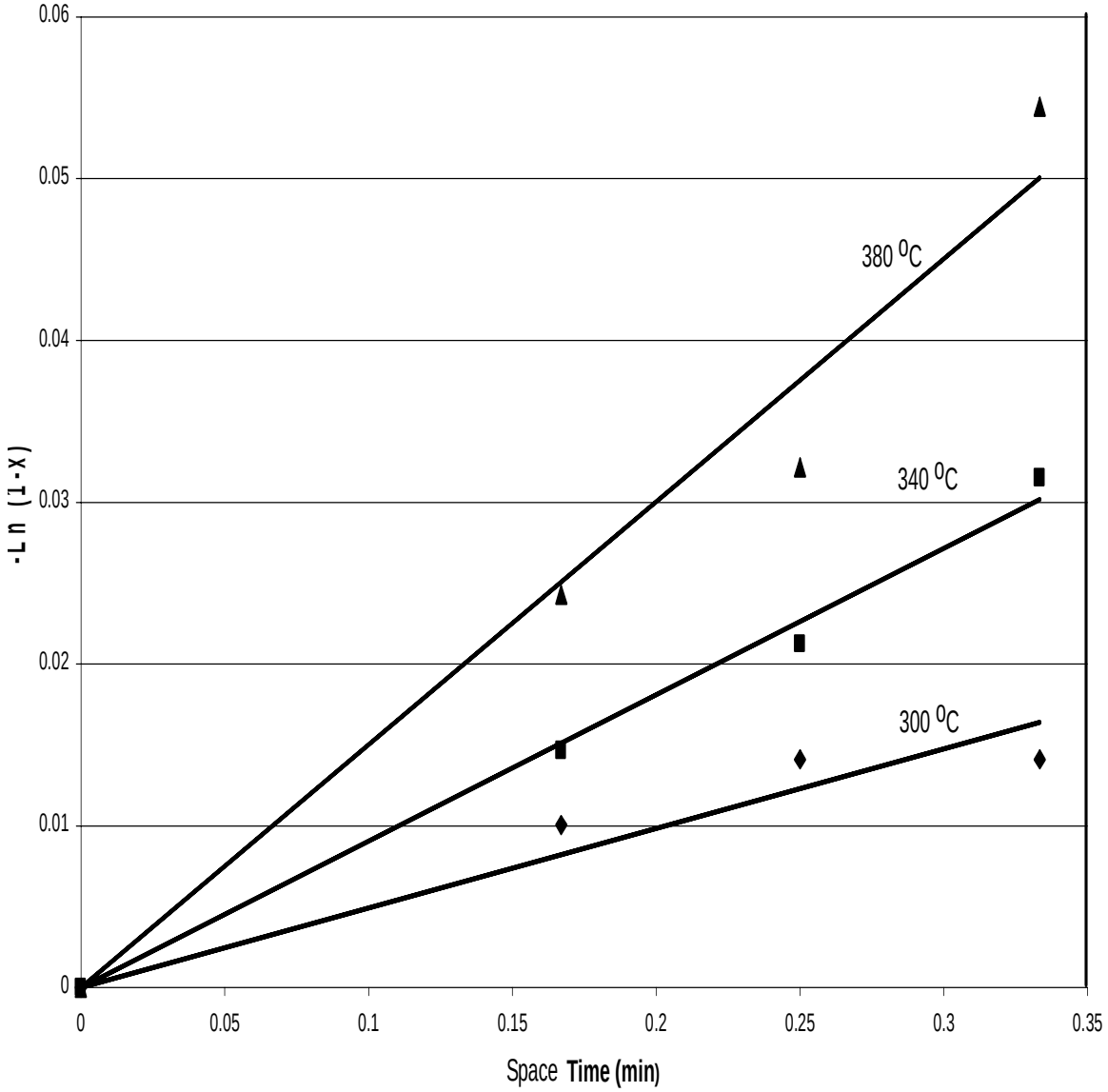
0.06
0.05
0.04
0.03
0.02
0.01
0
-Ln (1-X)
380 °C
340 °C
300 °C
0
0.05
0.1
0.15
0.2
0.25
0.3
0.35
Space Time (min)

Figure 3.15 : Rate of n-hexane cracking over the catalyst as a function of contact time at three different temperatures .

3.9 Activation Energy

The value of activation energies E_a was obtained from an Arhenius plot of -Ln k versus 1/T as shown in Figure 3.16 where the slope is equal to E_a/R and R is 8.314 joule/mole.K. The value of activation energies E_a was found to be 11.69 kcal/mole. Different values of activation energy has been reported in the literature, a low value of 14.6kcal/mole for n-hexane cracking over HZSM-5 was reported earlier by Borade et al [96] . For a variety of cracking catalyst Wang et a1 [97] reported values ranging from 15 to 30kcal/mole. It has been suggested that low activation energies for the cracking over a certain catalyst is an indication that the reaction rate was inhibited by the significant percentage of unexposed aluminosilicates. Another parameter that affect the activation energy is the acidity of zeolites on the walls where the more acidic the zeolites are, the more cracking there is and thus higher activation energy. Thus activation energy values for cracking catalysts is a combination of both diffusion and acidity strength. However in the case of our catalyst diffusion is enhanced since we have macropores connected through channels while the low value of 11.69 kcal/mole activation energy can be attributed to the fact that around 50% of the zeolite in the structure is of lewis acidity type since we have around 50% of the alumina in the octahedral fashion. In addition to that, TGA results showed that there is around 42% loading of alumino silicate in the 3 DOM carbon backbone, however not all

of the aluminosilicates are crystalline and exposed to the outer surface. The 3DOM Structure itself is microporous and significant percentage of the 42% loading is filling these micropores and remaining there as amorphous aluminosilicate since they are enclosed in a small volume where they can't form crystals. These alumina silicates are inaccessible, to hexane, leading to the diffusion constraint. Only after these micropores are filled, did zeolites started growing on the surface of the carbon. This justification can be supported by the fact that the grown zeolites remained on the walls of the carbon catalyst after calcination and didn't fall because they are anchored to the walls by the imbedded aluminosilicate.

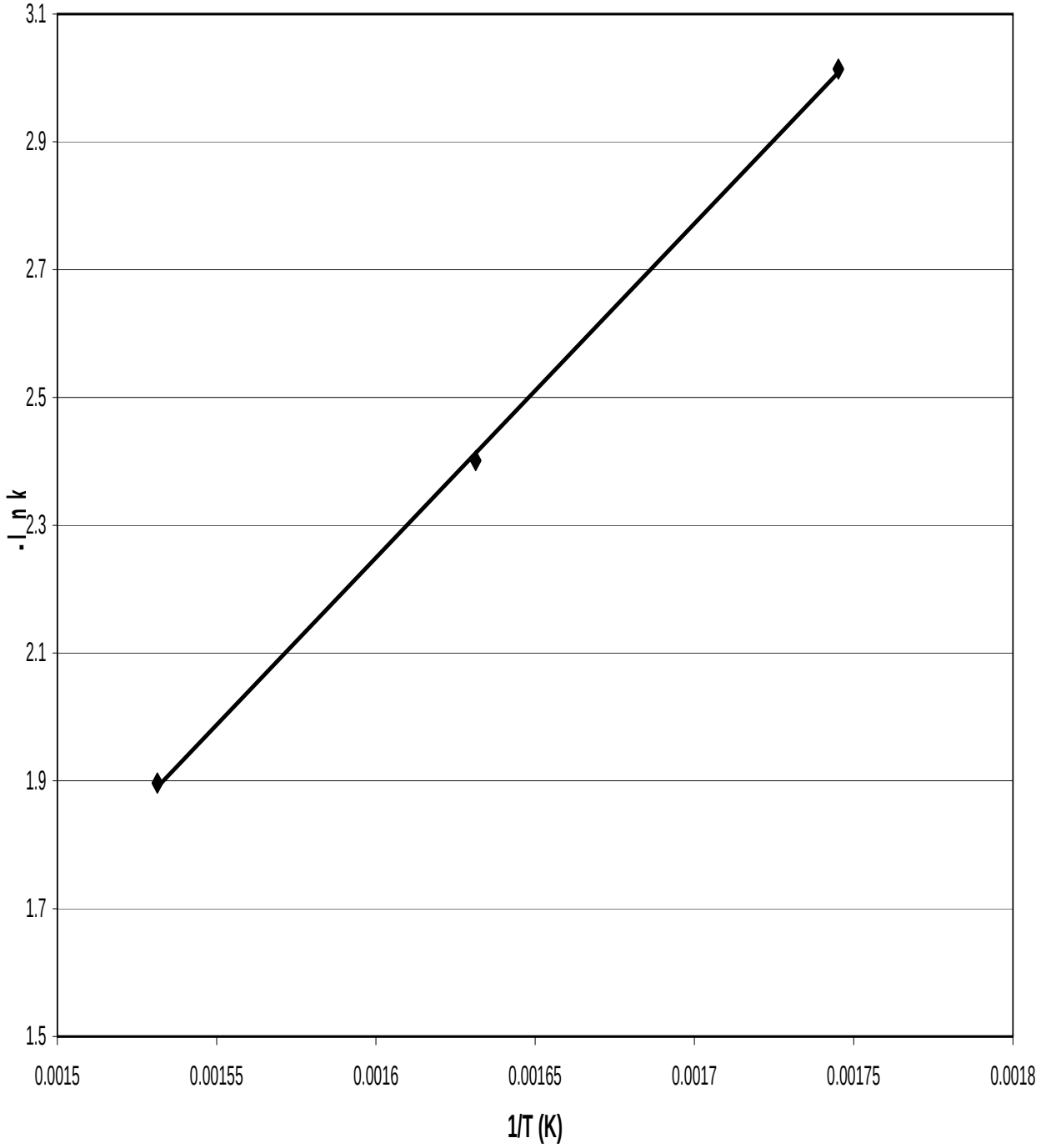
3.1
2.9
2.7
2.5
2.3
2.1
1.9
1.7
1.5
-ln k
0.0015
0.00155
0.0016
0.00165
0.0017
0.00175
0.0018
1/T (K)

Figure 3.16 : Plot of -Ln k versus 1/T .

3.10 Complete reaction and products collected

The complete reaction of polyethylene with zeolite coated carbon catalyst and polyethylene with powdered zeolites yielded both gaseous and liquid products analysis each in a different ratio and composition .

In addition to that TGA was used to study the influence of polymer (high density polyethylene) to catalyst ratio as shown in Figure 3.17a. The results presented in this figure shows that in the absence of the catalyst, complete degradation of the polymer took place at higher temperature (480 °C), while in the presence of the catalyst the polymer degradation occurred at lower temperatures (420-440 °C). In order to make sure that polymer degradation is due to the zeolite layer and not to the 3 DOM carbon itself, the same polymer to 3DOM carbon ratios were tested in TGA .As shown in Figure 3.17b polymer degradation for almost all polymer to 3 DOM carbon ratios took place at a temperature similar to that of blank polymer verifying that the lower degradation temperatures observed in Figure 3.17a are due to catalytic action of the zeolite layer coating the 3 DOM walls .

The complete reaction of 1g polyethylene with 0.5g powdered zeolites yielded 55% liquid products, 43 % gases, and 2% as coke in the zeolite .

The complete reaction of 1 g polyethylene with the 1.25 g zeolite coated carbon catalyst which is equivalent to 0.5 g zeolite in the catalyst yielded 51 % liquid products, 45 % gases, and 9 % as coke in the zeolite coated carbon catalyst.

The distribution of gaseous materials in the product of the two complete reactions is shown in Figure 3.17c as a function of weight percentage versus carbon number. As it can be noticed that the weight percentage of paraffins (mainly butane) in powdered zeolites is higher than in the zeolite coated carbon catalyst. The reason is that powdered zeolite is polar and enhances the adsorption of olefins on its surface which undergoes conversion by secondary reactions leading to the formation of coke and other smaller hydrocarbons which leads to its elution[98] .On the other hand the zeolite coated carbon catalyst showed higher weight percentage selectivity for olefins (mainly trans-butene) and the reason is that the catalyst backbone is carbon which is non polar thus favoring desorption of olefins from its surface which results in it elution as observed .

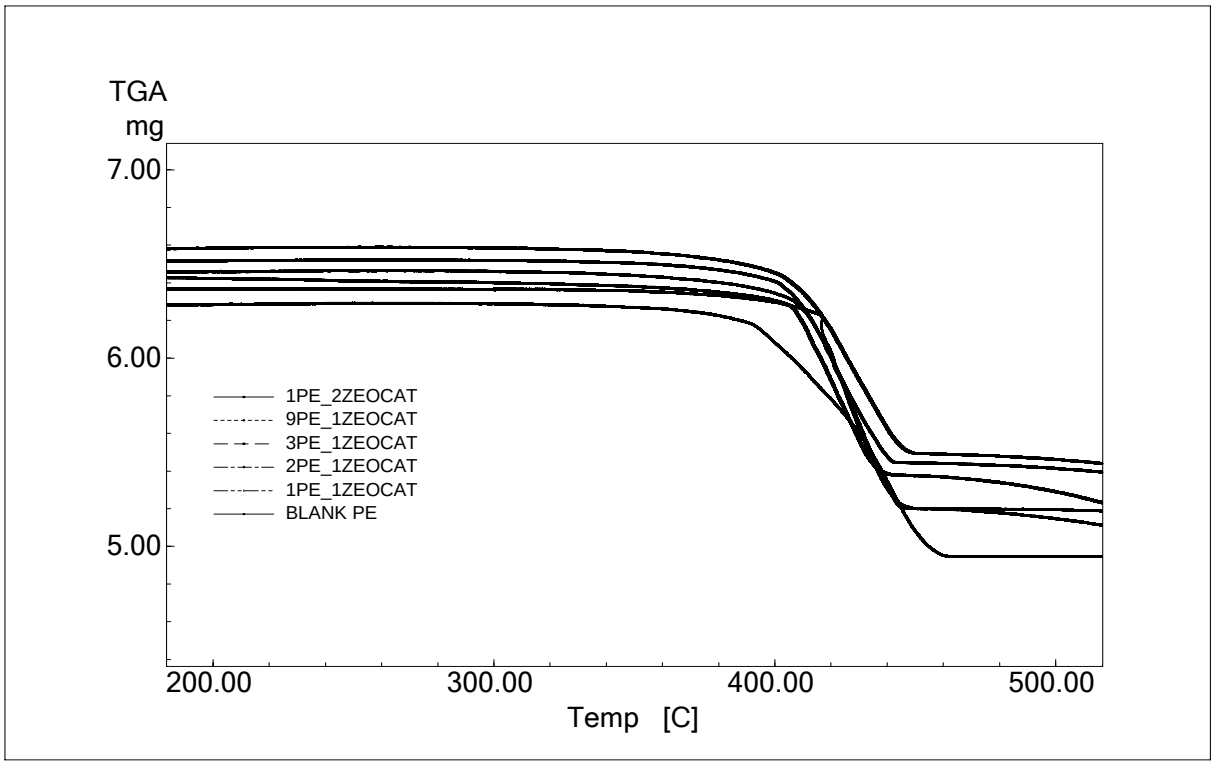

Figure 3.17a : TGA data for polymer and catalyst at different ratios .

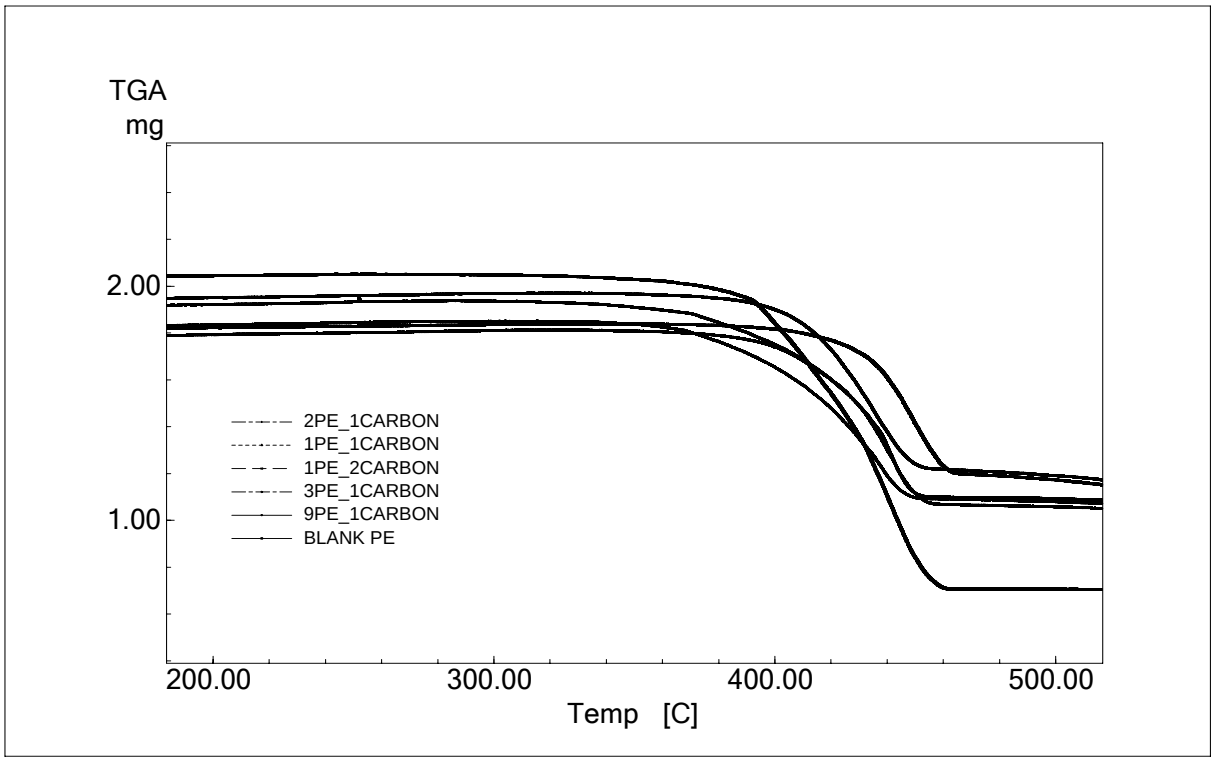

Figure 3.17b: TGA data for polymer and carbon at different ratios

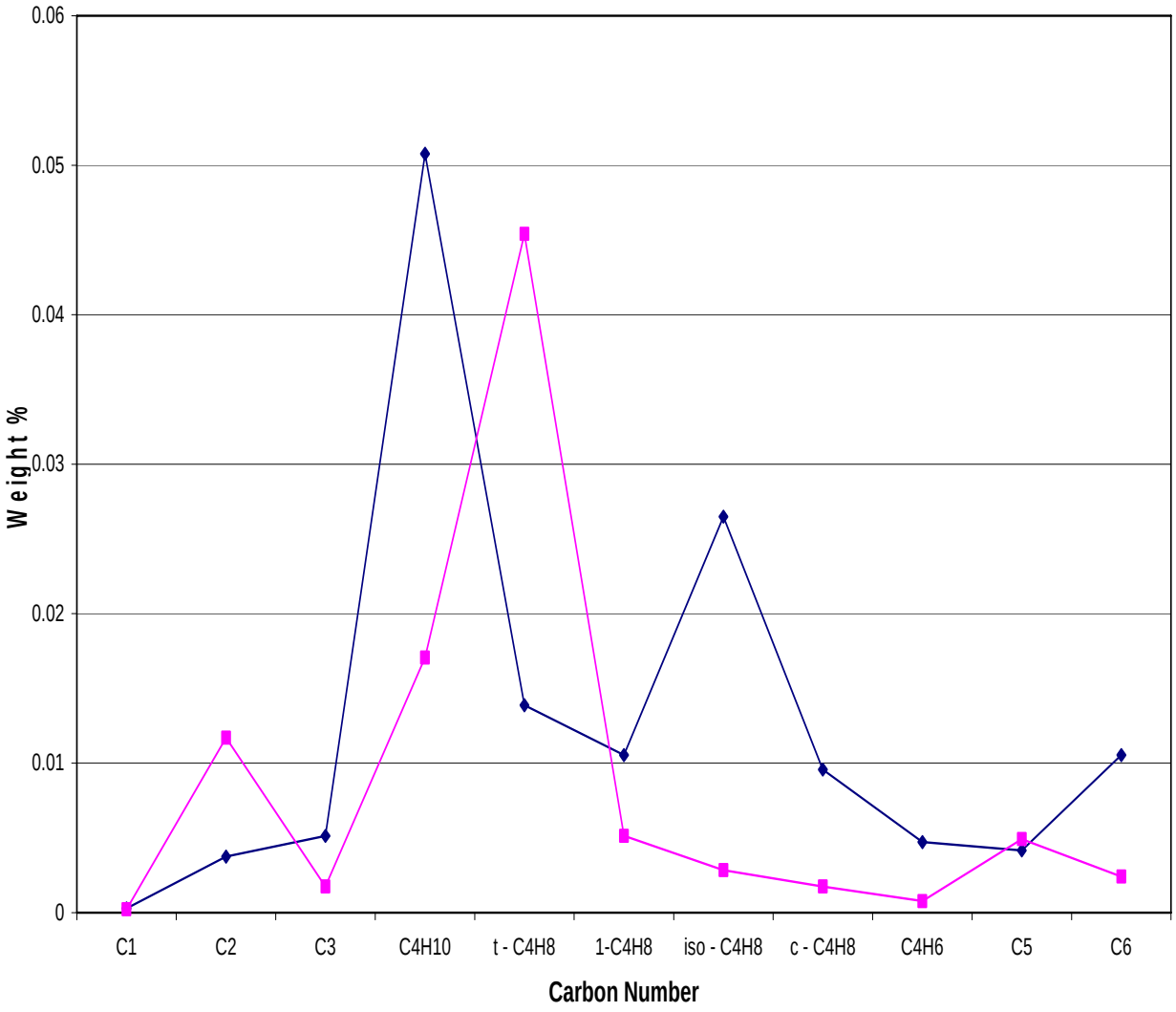

Figure 3.17c: Plot of weight percentage versus carbon number .

CH 4

CONCLUSION

4.1 Conclusion

A quest to grow nanoparticle zeolites on a three dimensional ordered macroporous (3DOM) carbon support was undertaken in this research**.** It started out by the preparation of a 3DOM carbon support from a poly (methyl methacrylate) monodisperse latex dispersion which were filtered and dried to act as a latex. Later this latex was soaked with a carbon precursor solution followed by filtering, drying and then calcination in order to produce 3 DOM carbon. Growth of nano particle zeolites in a uniform fashion on such a support was the challenge since carbon is hydrophobic and zeolites are hydrophilic. Such a process is not favored due to interaction mismatching, thus an interface of a polyelectrolyte multilayer system was introduced between the carbon and zeolites in order to change the hydrophobicity of the carbon surface and favor the interaction with zeolites aqeous, alkaline precursor. After modifying the carbon surface with a polyelectrolyte ,zeolites of nanoparticle sizes were grown hydrothermally in a uniform fashion. Later the as-synthesized zeolite coated carbon catalyst was calcined in an inert atmosphere in order to remove the tetra propyl structure directing agent from the zeolite pores. IR analysis was used to verify that the grown aluminosilicates are zeolitic with MFI morphology in the nanoparticle size range, TGA was used to acertain the amount of aluminosilicate loading in the 3 DOM carbon support, NMR was used to verify the alumina and silica

coordination in the framework, ICP was used to determine the silica to alumina ratio in the aluminsilicate, surface area measurements was used to verify that micropores are introduced into the macropore system, and SEM was used to verify that zeolites are grown on the walls. N-hexane cracking was used to test the acidity of the catalyst. Reaction results showed low activation energy value for n-hexane cracking due to the fact that not all of the aluminosilicates are crystalline and exposed to the surface .Finally catalytic activity of the catalyst was tested in a polymer degradation reaction which showed more selectivity towards olefins since olefins are polar and the catalyst backbone is carbon which is non polar thus favoring desorption of olefins from its surface which resulted in it elution.

REFERENCES

1. Stiles, A.B., *Catalyst supports and supported catalysts*. 1987: Butterworth publishers.

2. Seong -Su Kim, J. Shah, and T.J. Pinnavaia, *Colloida-Imprinted Carbons as Templates for the Nanocasting Synthesis of Mesoporous ZSM-5 Zeolite.* Chem. Mater, 2003. **15**: p. 1664-1668.

3. Zuxian Yang, Youngde Xia , and R. Mokaya, *Zeolite ZSM-5 with Unique Supermicroporous Synthesized Using Mesoporous Carbon as a Template.* Adv Mater, 2004. **16**: p. 727-732.

4. Yousheng Tao, et al., *Comparative Study on Pore Structures of Mesoporous ZSM-5 from Resorcinol -Formaldehyde Aerogel and Carbon Aerogel Templating.* J. Phys Chem .B, 2005. **109**: p. 194-199.

5. Boisen, A., et al., *TEM stereo -imaging of mesoporous zeolite single crystals.* CHEM COMMUN, 2003: p. 958-959.

6. Liu, Y. and T.J. Pinnavaia, *Aluminosilicate mesostructures with improved acidity and hydrothermal stability.* J.Mater .Chem, 2002. **12**: p. 3179-3190.

7. Uddin, M.D.A., and P.D. Stab., Poly. Degrad. Stab, 1997. **56**: p. 37.

8. Sakata, Y., M.D.A. Uddin, and A. Muto, J. Anal. Appl . Pyrol, 1999. **51**: p. 135.

9. Guisnet, M. and P. Magnoux, *Coking and Deactivation of zeolites , Influence of the pore structre.* Appl. Catal., 1989. **54**: p. 1.

10. Dwyer, J. and D.J. Rawlence, *Fluid Catalytic Cracking.* Chemistry. Catal Today, 1993. **18**: p. 487.

11. Dwyer, J. and D.J. Rawlence, *Fluid catalytic cracking : Chemistry.* Catal.Today, 1993. **18**: p. 487.

12. Naber, J., Stud. Surf. Sci. Catal., 1994. **84**: p. 2197.

13. Breck, D., New York: John Wiley and Sons., *Zeolite Molecular Sieves.* 1974.

14. Smirniotis, L.D. P.G., and E. Ruckenstein, *Composite Zeolite-Based Catalysts and Sorbents.* Cata. Rev.-Sci. Eng, 1999. **41(1)**: p. 43-113.

15. Holland, B.T., C.F. Blanford, and A. Stein, Science, 1998. **281**: p. 538-540.

16. Wijnhoven, J.E.G.J. and W.L. Vos, Science, 1998. **281**: p. 802-804.

17. C. J. H. Jacobsen, et al., J. AM. Chem. SOC, 2000. **122**: p. 7116.

18. C. Madsen and C.J.H. Jacobsen, CHEM .COMMUN, 1999: p. 673.

19. M Yamamura, et al., Zeoites, 1994. **14**: p. 643.

20. S. Mintova and T. Bein, Adv Mater, 2001. **13**: p. 1880.

21. http://www.bza.org/zeolites.html.

22. Meyer , W.M., D.H. Olsen, and Baerlocher, Ch. Zeolites, 1996. **17**: p. 1.

23. Weisz, P.B., Pure Appl . Chem, 1980. **52**: p. 2091.

24. Chen, N.Y. and W.E. Garwood Catal.Rev-Sci Eng, 1986. **28**: p. 185.

25. Holderich, W.F., Pure Appl. Chem, 1986. **58**: p. 1383.

26. Bekkum , H.V. and Kouwenhowen, Stud .Surf .Sci Catal, 1988. **41**: p. 45.

27. Goldstein , A.N., *Handbook of Nanophase Materials*, ed. M. Decker. 1997, New York.

28. Barrer, R.M., *Hydrothermal Chemistry of Zeolites.* Academic press :New York, 1982.

29. Ueda, S., et al., J .Phys Chem, 1984. **88**: p. 2128.

30. Ueda, S., N. Kargeyama, and M. Koizumi. in *Proc Int.Zeolite Conf ,6th*. 1984.

31. Szostak, R., et al. in *Proceedings of the Vll European Symposium on Materials and Fuid Sciences in Microgravity*. 1992. Brussels.

32. Persson, A.E., et al., Zeolites, 1994. **14**: p. 557.

33. Schoeman, B.J., J. Sterte, and J.E. Otterstedt Zeolites, 1994. **14**: p. 568.

34. Schoeman, B.J., J. Sterte, and J.E. Otterstedt Porous Mater, 1995. **1**: p. 185.

35. Persson, A.E., et al., Zeolites, 1995. **15**: p. 611.

36. Jacobs, P.A., et al., J .Phys Chem B, 1998. **102**: p. 2633-2639.

37. T.A.M. Toweny, et al., Zeolites, 1994. **14**: p. 162.

38. O. Regev , et al., Zeolites, 1994. **14**: p. 314.

39. J. Dougherty , L.E. Iton, and J.W. White, Zeolites, 1995. **15**: p. 640.

40. K.F.M.G.J. Scholle, et al., Appl. Catal., 1985. **17**: p. 233.

41. J. Dougherty, L.E. Iton , and J.W. White, Zeolites, 1995. **15**: p. 640.

42. B.J.Schoeman, Zeoites, (Accepted).

43. Scoeman, B.J., Microporous Materials, 1997. **9**: p. 267-271.

44. J. A. Martens, et al., J .Phys Chem B, 199. **103**: p. 4972-4978.

45. R. Ravishankar, et al. in *proceedings of the 12th International zeolite conference*. 1999. Pennsylvania.

46. Flanigen , E.M., et al., Nature of Initial Polymer Reactions, Pattern of Formation of Gas and Liquid products, and Temperature Effects, 1978. **271**: p. 512.

47. Derouane, E.G., et al., Appl. Catal., 1981. **1**: p. 201.

48. Testa, F., et al., Zeolites, 1997. **18**: p. 106.

49. Martens, J.A., et al., *Characterization of Nanosized Material Extracted from Clear Suspensios for MFI zeolite Synthesis* . J .Phys Chem .B, 1999. **103**: p. 4960-4964.

50. Kinrade S.D, et al., Inorg .Chem, 1998. **37**: p. 4278.

51. Chang. C. D and Bell. A.T, Catal.Lett, 1991. **8**: p. 305.

52. McMullan. R. K, M. Bonamico, and Jeffery. G. A, J .Phys Chem, 1963. **39**: p. 3295.

53. Kokotailo, G.T., et al., Nature, 1978. **272**: p. 437.

54. T, I., *zeolites synthesis, ACS Symp.Ser ,398 (Eds .M.L , Occelli and H.E Robinson) Washington , DC.* Am .Chem.Soc, 1989: p. 479.

55. Sakeel Ahmed and M.Z.A. Faer, Zeolites, 1996. **17**: p. 373- 380.

56. Baerlocher. C. H, W.M. Meier, and D.H. Olsen, Atlas of zeolite framework types ,Science, 2001.

57. kresge, C., T,, et al., Nature, 1992. **359**: p. 710-712.

58. Ogura. M, et al., Chem. Lett, 2000: p. 882-883.

59. Groen . J C , P.-R. J, and Peffer. L.A.A, Chem. Lett, 2002: p. 94-95.

60. Jacobsen. C.J.H, et al., J. AM. Chem. SOC, 2000. **122**: p. 7116-7117.

61. Schmidt, I., et al., Chem .Mater, 2001. **13**: p. 4416-4418.

62. Zhang. B. J, Davis. S. A, and M. S, Chem .Mater, 2002. **14**: p. 1369-1375.

63. Van Der Pol. A. J. H. P, Verduyn. A. J, and Van Hoff. J. H.C, Appl. Catal., 1992. **92**: p. 113-130.

64. Rajagopalan. K, Peters. A. W, and Edwards. G.C, Appl. Catal., 1986. **23**: p. 69-99.

65. Camblor. M. A, et al., Appl. Catal., 1989. **55**: p. 65-74.

66. Camblor. M. A, et al., J Catal, 1998. **179**: p. 537-547.

67. Yamamura. M, et al., Zeolites, 1994. **14**(643-649).

68. Jacobs, P.A., E.G. Derouane, and Weitkamp. J, J. Chem. Soc.Chem.Commun, 1981: p. 591-593.

69. Schmidt, I., Madsen. C, and C.J.H. Jacbson, Inorg .Chem, 2000. **39**: p. 2279-2283.

70. Lee. J, Sohn. K, and Hyeon. T, J. AM. Chem. SOC, 2001. **123**: p. 5146-5147.

71. Li. Z . J and J. M, J. AM. Chem. SOC, 2001. **123**: p. 9208-9209.

72. Schuth. F, Chem .Mater, 2001. **13**: p. 3184-3195.

73. ThomasJ. Pinnavaia, Seong-Su Kim , and J. Shah, *Colloid Imprinted Carbons as Templates for the Nanocasting Synthesis of Mesoporous ZSM-5 Zeolite.* Chem .Mater, 2003. **15**: p. 1664-1668.

74. Robert Mokaya , Zhuxian Yang, and Y. Xia, Adv Mater, 2004. **16**: p. 727-732.

75. kaneko, K., et al., J .Phys Chem B, 2005. **109**: p. 194-199.

76. Astrid Boisen , et al., *TEM stereo-imaging of mesoporous zeolite single crystals.* CHEM .COMMUN, 2003: p. 958-959.

77. ThomasJ. Pinnavaia and Y. Liu, J.Mater .Chem, 2002. **12**: p. 3179-3190.

78. Beck. J .S, et al., J. AM. Chem. SOC, 1992. **114**: p. 10837-10843.

79. Zhao. D, et al., Science, 1998. **179**: p. 548-552.

80. Antonietti. N, et al., Adv Mater, 1998. **10**: p. 154-159.

81. Imhof. A and Pine. D. J, Nature, 1997. **389**: p. 948-951.

82. Imhof. A and P.D. J, Adv Mater, 1998. **10**: p. 697-700.

83. Velev. O. D, et al., Nature, 1997. **389**: p. 447-448.

84. Andreas Stein, et al., Chem. Mater, 1999. **11**: p. 795-805.

85. Andreas Stein, et al., Chem Mater, 2000. **12**: p. 1134-1141.

86. Songip, A.R., et al., *Test o screen catalysts for reforming heavy oil from waste plastics.* Appl. Catal., 1993. **22**: p. 153.

87. Songip, A.R., et al., *Kinetic studies for catalytic craking of heavy oil from waste plastics over REY Zeolite.* Energy Fuels, 1994. **8**: p. 131.

88. Uemichi, Y., et al., *Product Distribution in Degradation of polypropylene over Silica-Alumina and CaX Zeolite Catalysts.* Bull .Chem. Soc .Jpn, 1983. **56**: p. 2768.

89. Audisio. G, et al., *Catalytic degradation of polyolifens.* Makromol. Chem - Macromol. Symp, 1992. **57**: p. 191.

90. Garforth. A A, et al., *Production of hydrocarbons by catalytic degradation of high density polyethylene in a laboratory Fuidized -Bed reactor.* Appl. Catal.A, 1998. **169**: p. 331.

91. John Dwyer, George Manos, and A. Garforth, *Catalytic Degradation of High Density Polyethylene on an Ultrastable -Y Zeolite. Nature of Initial polymer reactions .Pattern of formation of gas and liquid Products , and Temperature Effects* . Ind. Eng. Chem. Res, 2000. **39**: p. 1203-1208.

92. Seo, G., Young San You, and J.-H. Kim, *Liquid-phase catalytic degradation of polyethylene wax over MFI zeolites with different particle sizes.* Polymer Degradation and Stability, 2000. **70**: p. 365-371.

93. Jacobs. P, Derouane. E.G, and W. J, J. Chem. Soc.Chem.Commun, 1981. **591**.

94. Jansene , J.C., Vander Gaag F. F , and Beckkum . H, Zeoites, 1984. **4**: p. 369-372.

95. Jacos, P.A., Bayer. H . K , and V. j, Zeoites, 1981. **1**: p. 161.

96. Borade, R.B., et al., Applied Catal, 1984. **13**: p. 27.

97. Wang, et al., J. Catal., 1979. **60**: p. 140.

98. Manos, G., A. Garforth, and J. Dwyer, Ind. Eng. Chem. Res., 2000. **39**

VITAE

Name: Toufic Nabil Aridi

Nationality: Lebanese

Birth Date:21/11/1979

B.S. Degree in Chemistry : Lebanese University, 2001.

M.S. Degree in Chemistry: King Fahd University of Petroleum and Minerals, 2006.

Email: tnttoto@hotmail.com